Fall 2015

An objective CT-based method for quantifying articular fracture severity : clinical application in multiple joints

Kevin Nathaniel Dibbern
University of Iowa

AN OBJECTIVE CT-BASED METHOD FOR QUANTIFYING ARTICULAR FRACTURE SEVERITY: CLINICAL APPLICATION IN MULTIPLE JOINTS

by

Kevin Nathaniel Dibbern

A thesis submitted in partial fulfillment
of the requirements for the Master of Science
degree in Biomedical Engineering in the
Graduate College of
The University of Iowa

December 2015

Thesis Supervisor: Associate Professor Donald D. Anderson

Graduate College
The University of Iowa
Iowa City, Iowa

CERTIFICATE OF APPROVAL

_____

MASTER'S THESIS

_____

This is to certify that the Master's thesis of

Kevin Nathaniel Dibbern

has been approved by the Examining Committee for
the thesis requirement for the Master of Science degree
in Biomedical Engineering at the December 2015 graduation.

Thesis Committee: _____
Donald D. Anderson, Thesis Supervisor

_____
Nicole M. Grosland

_____
Joseph M. Reinhardt

_____
Tae-Hong Lim

_____
J. Lawrence Marsh

ACKNOWLEDGEMENTS

First and foremost, I would like to thank my research supervisor Dr. Don Anderson for his guidance and continued support during my time in the Orthopaedic Biomechanics Lab. Additionally, I would like to thank him and all those who contributed to the prior research on fracture severity assessment in the lab for their substantial contributions. Dr. Anderson provided funding for my research through a grant from the NIH. I would also like to thank the Biomechanics Lab itself, with a special thanks to Andrew Kern for his help in the development of this project and guidance in the lab. Furthermore, I thank my family and friends for their support.

ABSTRACT

Adequately assessing injury severity is critical in treating articular fractures. Severity assessment is used to inform clinical and surgical decision making through anticipation of patient outcomes. The assessments generally involve interpreting radiographs or CT image data. In recognition of the poor reliability of existing clinical severity assessments, objective severity metrics have been developed that are firmly rooted in mechanics and provide capable alternatives for use in research, where reliable data is paramount. Their broader clinical utility remains to be established.

An existing CT-based method for determining the energy expended in a bone fracture was extended to facilitate its use in more fracture types. Its utility in different articular joints was evaluated. Specifically, the severities of articular fractures of the proximal tibia (plateau), of the distal tibia (plafond), and of the calcaneus were compared with present clinical severity metrics, patient outcomes, and/or surgeon rankings of severity. Differences in the fracture energies in the different joints were also compared.

The objective fracture energy metric compared favorably with present clinical severity metrics. The fracture energies for fractures of the tibial plateau had between 71% and 78% concordance with surgeon rankings of severity. The calcaneal fracture energies had a 75% concordance with the present clinical standard. Fracture energy was also predictive of later radiographic indicators of post-traumatic osteoarthritis.

The fracture energy metric is a capable tool for analyzing fracture severity in various joints. Fracture energy correlated well with outcomes and present clinical gold standards for severity assessment. The methods for assessing fracture energy described are highly useful for orthopaedic research and have potential as an important clinical tool.

PUBLIC ABSTRACT

Adequately assessing injury severity is critical in treating articular fractures. Severity assessment is used to guide clinical and surgical decision making through anticipation of clinical outcomes. The assessments generally involve interpreting medical image data. The poor reliability of existing clinical severity assessments led to the development of objective severity metrics that have proven capable alternatives for use in research, where reliable data is paramount.

A new means for measuring the energy expended in fractures was developed for objectively assessing injury severity. Its capability in different anatomical regions was evaluated. Specifically, it was compared with present clinical metrics, patient outcomes, and/or surgeon rankings of injury severity in the knee, ankle, and in the calcaneus. The different distributions of fracture energies in these different regions were also compared.

The objective fracture energy metric compared favorably with present clinical metrics. The fracture energy metric in the tibial plateau had between 71% and 78% concordance with surgeon rankings of severity. The calcaneal fractures analyzed had a 75% concordance with the present clinical standard. The fracture energy was also predictive of later development of post-traumatic osteoarthritis.

The fracture energy metric is a capable tool for analyzing injury severity in various joints. This utility had previously been shown in fractures of the tibial plafond, but improvements have allowed for extension to other joints and bones. The resulting severity metric shows good correlation with outcomes and present clinical gold standards for severity assessment. The methods for assessing fracture energy developed are highly useful for orthopaedic research and have potential to be an important clinical tool.

TABLE OF CONTENTS

LIST OF FIGURES

CHAPTER 1: INTRODUCTION AND BACKGROUND

1.1 Fracture severity assessment and its significance

Adequately assessing injury severity is critical in treating fractures of articular joints. Severity assessment informs clinical and surgical decision making by enabling the prediction of patient outcomes. In the case of articular fractures, the risk of later post-traumatic osteoarthritis (see §1.2 below) is a major concern. Reliable injury severity assessment is necessary for meaningful comparisons of different treatment options. For these reasons, among others, the poor reliability of existing clinical severity assessments led to the development of objective fracture severity metrics that have proven capable alternatives for use in research, where reliable data are paramount[3-8].

Fractures are classified using different schemes in orthopaedics to convey information about them. The most useful clinical fracture classifications are largely based on categorizing injuries according to various features of articular fractures that are readily identifiable on radiographs or CT scans. Typically these features include: the location of the fractures, the number of fragments, the amount of fracture displacement, and the anticipated degree of surgical difficulty in treating them[9]. Perhaps not surprisingly, subjective assessment of these features can vary between physicians and lead to the aforementioned poor reliability. Prior methods that sought to obviate these problems focused on identifying and quantifying objective CT-based metrics of fracture severity, such as the fracture energy, the degree of articular comminution, and the amount of fracture displacement [3, 4, 10, 11]. The focus of the present work remains on quantifying the joint injury by measuring the amount of energy transmitted through the

articular surface in the fracturing of bone, but an additional aim is to broaden the clinical utility and practicality of using these methods.

Prior objective CT-based methods for obtaining these metrics succeeded in fulfilling the need for increased reliability, but they lacked broader applicability; constrained by either relying on the existence of CT scans of the intact contralateral limb or having a suitable anthropometric surrogate for the intact limb [3-5, 11]. These limitations were undesirably compounded by the sometimes abstruse nature of expedited surrogate metrics that were developed. In contrast to this, traditionally embraced fracture severity metrics have stood the test of time because of their broad applicability and ability to be easily understood. The AO classification of long bone fractures exemplifies these successes, possessing easily identifiable classification criteria and measures that can be applied and understood in any joint[9]. The goal of the present work is to extend existing methods to emulate these qualities with an objective metric that can be utilized more broadly for research and clinical application.

Accomplishing the goal of creating a more utilitarian methodology also requires that the metric be fairly expedient and simple to use. This thesis aims to incorporate the broad applicability and plain features that have been staples of widely adopted clinical fracture classification systems while improving upon their reliability. A major benefit of the methods proposed herein is that they use measures of a physically meaningful concept; the quantity of energy absorbed by bone in fracture production. This aids researchers in the understanding and interpretation of severity results and is important as it can be difficult to assess the quality of a newly developed metric. The challenge of assessing the new metric, lacking any other gold standards with which to compare, was

undertaken by analyzing results alongside previously validated fracture energy measures and the present clinical gold standard of surgeon opinion. Expediting assessment methods that produce direct measures of fracture severity was achieved by implementing a trained machine learning classifier to enable the automated identification of and provide more accurate discrimination of fractured bone surfaces working from segmentations. In addition, a 3d graphical user interface was developed to finalize the identification of de novo fracture surface in bone models segmented from CT scans.

This thesis details the development of a fracture severity assessment methodology that is capable of being applied to any articular fracture. It addresses prior issues with reliability, utility, and clarity by proposing an objective CT-based method to quantify fracture liberated surface area and to determine the quantity of energy absorbed by the bone in producing a fracture. This study opens the possibilities for use of such a robust, expeditious, and versatile metric in a diverse set of research and clinical applications where objective assessment of injury severity is required.

1.2 Post-Traumatic Osteoarthritis:

Post-traumatic osteoarthritis (PTOA) is a debilitating, degenerative condition of the joints that follows a traumatic injury. It is most common and likely following a fracture involving a joint. PTOA results in impairment equivalent to that of end stage renal disease or heart failure, and it affects a large percentage of those who have suffered significant joint injuries[12]. With present care, 44% of patients having sustained an intra-articular proximal tibia (plateau) fracture will develop knee OA, while greater than 50% of those with intra-articular distal tibia (plafond) fractures will develop OA[13]. By five to eleven years after a tibial plafond fracture, the incidence of ankle OA is 74%. [14] While the understanding of the etiology of PTOA has improved in recent years, patient-specific prognoses are, however, still "largely speculative."[15]

The extent of damage to the joint and the likelihood that the joint will later develop PTOA following a joint injury is, at least in part, a function of the initial mechanical insult to the articular surface. As insult severity varies and strongly influences the probability of PTOA development, different injury severities necessitate different treatment options. For example, in more severe injuries, a primary fusion or arthroplasty could spare the patient future surgeries, because the joint would be expected to rapidly develop PTOA regardless of surgical intervention. Presently, fracture classification systems fill the role of guiding surgical management in such situations. While these classifications are currently the standard of care, clinical decision making could be further improved with an objective fracture severity metric that could be expeditiously and easily obtained for a variety of fracture types.[15-17]

1.3 The Tibia:

As previously detailed, the ability to better predict the onset of PTOA is of particular import in the assessment of fracture to an articular surface. An objective CT-based fracture severity metric was previously shown to improve such predictions in the distal tibia [10]. The CT-based methodologies proposed herein would expand use to the proximal tibia, among other joints, in pursuit of application to any articular fracture. The tibia articulates proximally with the femur to form the knee joint and distally with the talus to form the ankle joint. Fractures through the proximal and distal articulating surfaces of the tibia can be particularly devastating injuries that are predisposed to PTOA and joint degeneration. Therefore, enhanced predictive capabilities regarding injury outcomes involving these joints would have a significant impact on patient care.

1.3.1 Anatomy of the Knee Joint:

The proximal portion of the tibia, often referred to as the tibial plateau, comprises the distal-most portion of the knee joint. The knee is the weight-bearing joint most often affected by OA[18]. It consists of two bony articulations: the patellofemoral joint and the tibiofemoral joint. The tibiofemoral joint is the primary weight-bearing joint in standing, knee flexion, and normal gait. The two condyles of the distal femur articulate with two distinct surfaces on the tibial plateau, separated into medial and lateral compartments by a bony protrusion known as the tibial spine. The medial compartment has the largest contact area and typically carries the larger load. The lateral compartment is shallower and possesses less bony stability, relying instead on the substantial soft tissue structures of the knee for stability [18, 19].

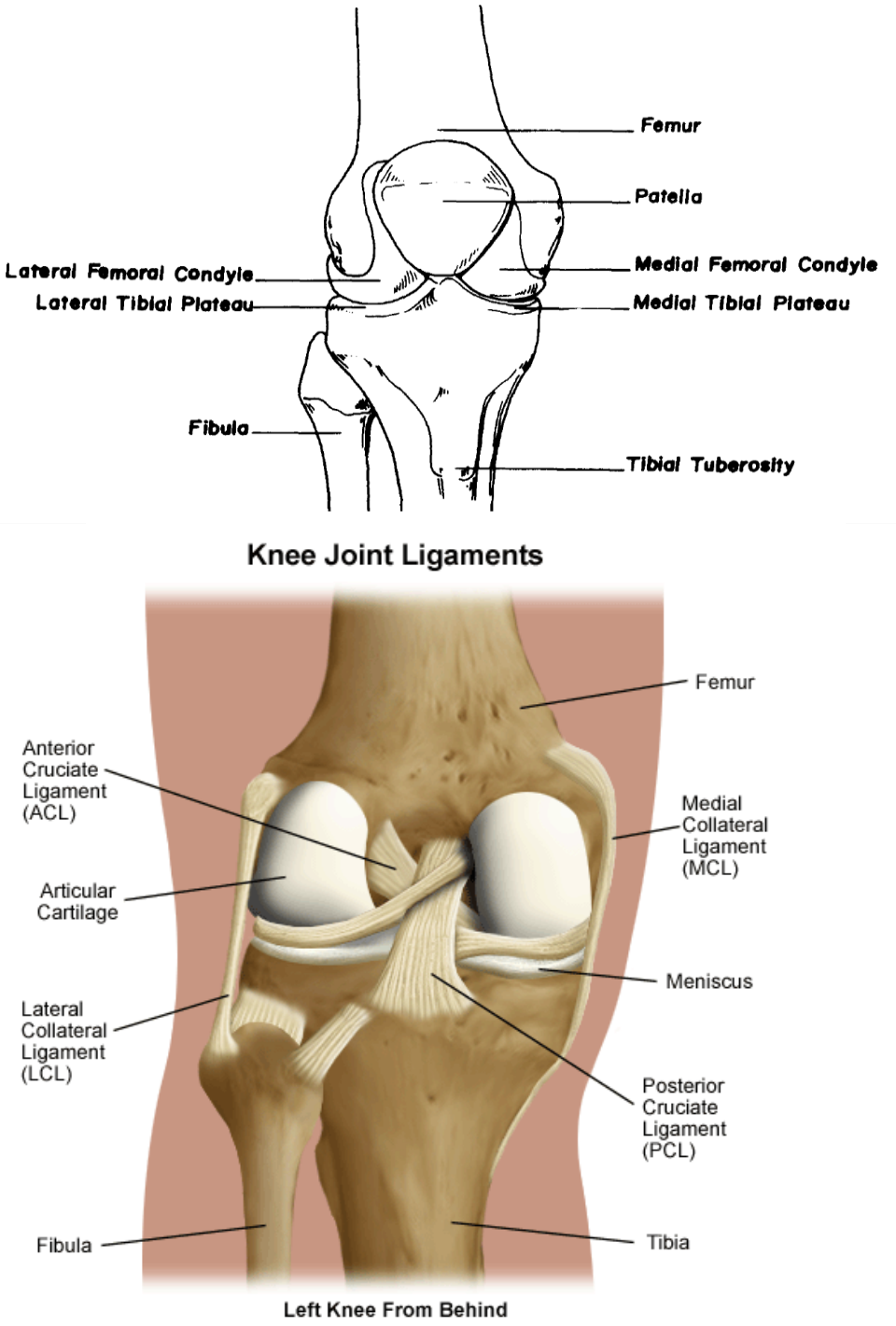

Figure 1-1: Anatomy of the proximal tibia [20, 21].

The soft tissues relied upon for stability in the knee include a fibrocartilaginous meniscus, five strong ligaments, and the patellofemoral contact. The anterior cruciate, posterior cruciate, medial collateral, and lateral collateral ligaments all restrain motion to prevent excessive translation of the tibia. These ligaments attach to the tibia as shown in Figure 1-1. The popliteofibular ligament (not labeled) resists posterolateral rotation of the tibia with respect to the femur adding to the soft tissue constraints afforded by the other ligaments. The meniscus contributes a substantial portion of load carriage across the joint, and damage to it or any of the surrounding soft tissue structures can be a significant factor in OA development [20, 22].

1.3.2 Anatomy of the Ankle Joint:

The ankle is comprised of the distal portions of the tibia and fibula articulating over the talus. The distal portion of the tibia is often referred to as the tibial plafond (or, interchangeably, the tibial pilon). Plafond, the French word for ceiling, is typically used to describe a vaulted or domed structure. Anatomically, this refers to the "dome" made over the talus by the distal tibia, its medial malleolus protrusion, and the fibula on the lateral side. In contrast with the knee, this bony anatomy makes a robust construct for articulation without requiring much contribution from the associated soft tissues.

The tibiofibular ligament, forming the syndesmosis joint, is the most important soft tissue structure in the ankle. It constrains the fibula relative to the tibia to create the proximal-most portion of what is effectively a mortise and tenon joint (as seen in Figure 1-2). Additional ligamentous stability is afforded by the four robust ligamentous structures encapsulating the joint.

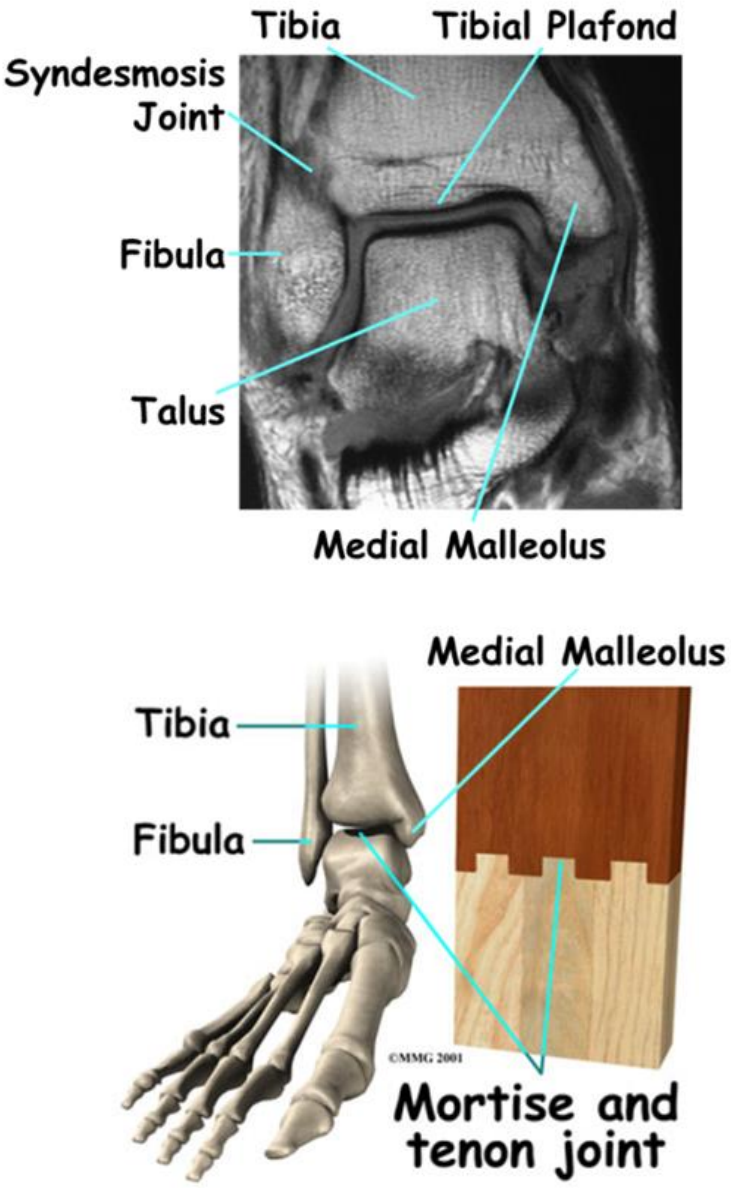

Figure 1-2: Anatomy of the Distal Tibia
[Rosenberg, Z.S., J. Beltran, and J.T. Bencardino, *From the RSNA refresher courses - MR imaging of the ankle and foot.* Radiographics, 2000. 20: p. S153-S179.]

1.3.3 Tibial Plateau Fractures

1.3.3.1 Description

Fractures of the tibial plateau are relatively uncommon, representing approximately 1% of all fractures. The circumstances that cause these fractures can vary greatly in the energy involved and the mechanism, ranging from higher-energy motor vehicle accidents, mechanical falls (not due to fainting or seizure), and sports injuries to lower-energy mechanisms in osteoporotic bone. Fractures are typically caused by a varus or valgus force combined with an axial loading. This force typically results in impaction or cleavage of the lateral or medial plateau. As the medial plateau is larger and typically stronger than the lateral plateau, fractures are more commonly found in the lateral plateau (55-70% of total incidence). Although rarer, fractures of the medial plateau (10-23% of total incidence) and of both plateaus (10-30% of total incidence) are considered to be higher-energy and more severe injuries.[22]

Outcomes of tibial plateau fractures have been shown to be largely dictated by initial injury severity, as judged by clinical classification systems[23]. Another important factor in these outcomes is the degree of ligamentous instability and the damage to the meniscus,[22] two factors that are beyond the scope of the current work.

1.3.3.2 Classification

The Schatzker and AO/OTA classification systems are the most commonly utilized for classifying fractures of the proximal tibia. The Schatzker classification system (Figure 1-3) was developed as a method for identifying groups of fractures with distinct pathomechanical and etiological factors[24]. This system has well established clinical

utility in guiding treatments and predicting outcomes[25]. The AO/OTA classification system (Figure 1-4), on the other hand, seeks to categorize fractures based upon their morphological characteristics in order of increasing severity, where severity "implies anticipated difficulties of treatment, the likely complications, and the prognosis."[9, 26] Where the Schatzker classification seeks to categorize intra-articular fractures, the AO/OTA Classification system encompasses a broader set of fractures.

The AO/OTA classification consists of: Type A, nonarticular fractures; Type B, partial articular fractures; and Type C, complete articular fractures. These are further subdivided, as shown in Figure 1-4, by increasing severity into subtypes 1, 2, and 3.The Schatzker classification, shown in Figure 1-3, consists of six categories denoted I-VI: class I fractures are lateral split type fractures without depression; class II fractures have a lateral split with depression; class III fractures are central depression fractures; class IV fractures are split medial plateau fractures; class V fractures are bicondylar in nature; and class VI are bicondylar with metadiaphyseal extension.

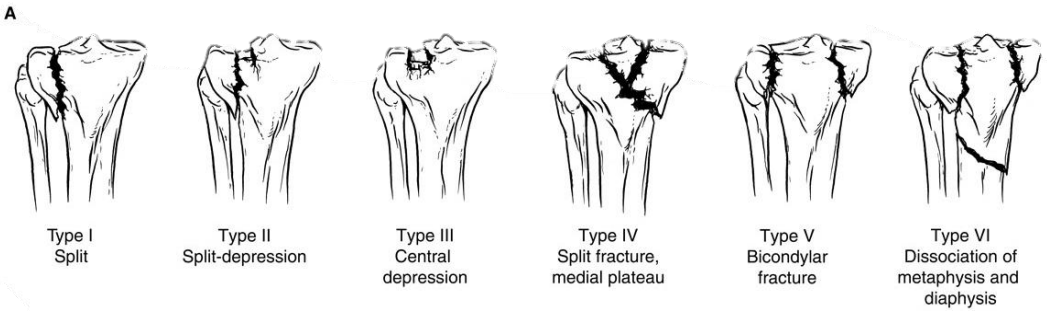

Figure 1-3: Schatzker Classification of Tibial Plateau Fractures. Developed to identify and group fractures with distinct pathomechanical and etiological factors, its ordering from Type I to Type VI reflects injuries that are increasingly challenging to treat. [27]

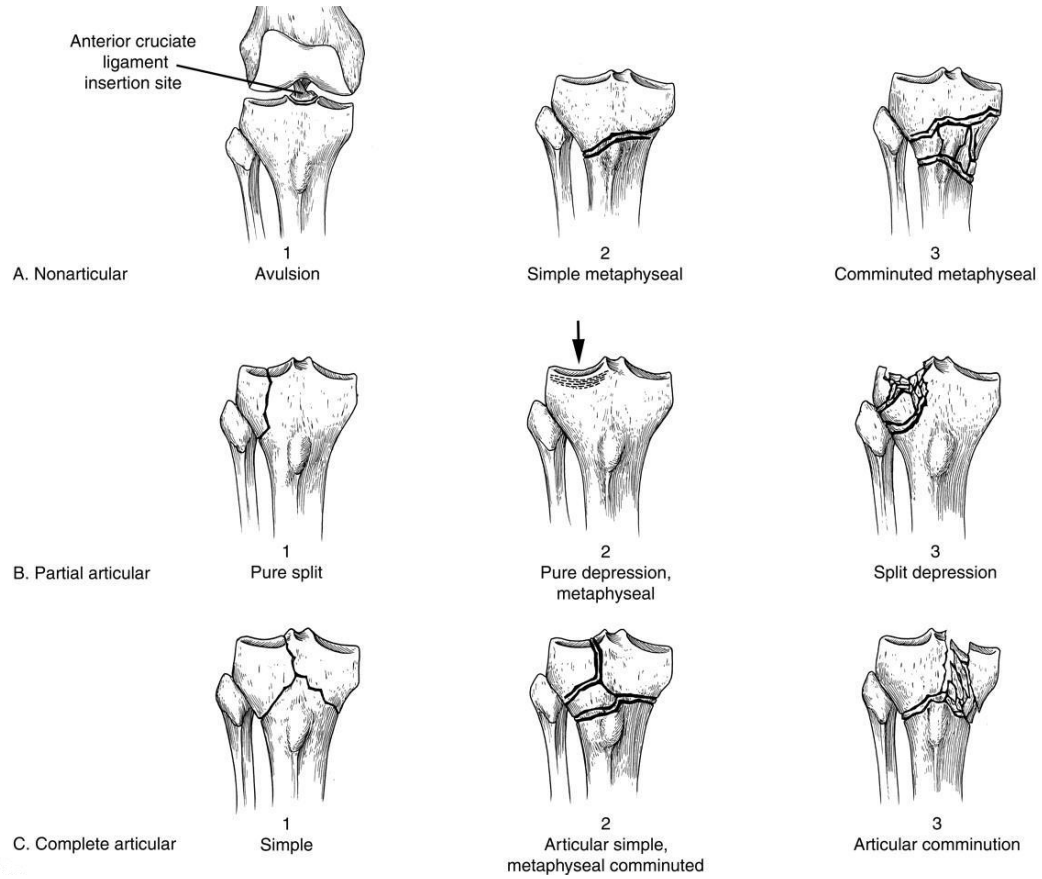

Figure 1-4: AO/OTA Classification of Tibial Plateau Fractures. It was created as a means for standardizing descriptions of fractures for research and communication. [27]

1.3.4 Tibial Plafond Fractures

1.3.4.1 Description

Fractures of the plafond are rare injuries representing less than 1 percent of lower extremity fractures and only 3-10% of tibial fractures[28-31]. Despite their rarity, they represent some of the most difficult fractures in the lower extremity to treat and are often associated with a high degree of soft tissue injury. There are typically two types of plafond injury: those arising from large axial impact forces, and those arising from torsional forces. The axial impact injuries occur when the talus is driven into the tibial plafond initiating a fracture pattern that extends from the plafond up the tibial shaft. These types of forces can stem from high energy falls from height, motor vehicle collisions, and other axially compressive injuries. The torsional type of fracture can produce less-complex, lower energy patterns that have large bone fragments and minimal impaction. In contrast, high energy compression injuries can have many smaller fragments known clinically as severe comminution, impaction of these and larger fragments, as well as damage to articular cartilage. Energy is often anecdotally related to injury severity due to these relationships between energy and bone fragment size, as larger fragments resulting from lower energy fractures are often easier to reduce with fracture fixation hardware. As the quality of surgical reduction is likely to increase with these improved methods, so are patient outcomes as the severity of the injury sustained and the quality of articular reduction assessed by orthopaedic surgeons have been found to be strongly correlated with PTOA [32].

This establishes a major component of the relationship between fracture energy, clinical injury severity assessment, and patient outcomes. It also serves to demonstrate

why plafond fractures are of particular import to the study of severity assessments as they can be used as predictive landmarks with which capabilities can be measured.

1.3.4.2 Classifications

There are two commonly utilized fracture classification systems in the distal tibia: the AO/OTA classification and the Ruedi-Allgower system. The AO/OTA classification (figure 1-5) consists of types A through C and a number, 1 through 3, reflecting increasing severity. It is a part of the larger AO/OTA classification of long bone fractures [9]. AO/OTA type A fractures are distal tibial fractures in the metaphysis without intra-articular extension. Type A1 fractures are simple, A2 fractures are comminuted, and A3 fractures are severely comminuted. Similarly, AO/OTA type B fractures are partial articular fractures categorized as B1 for pure split, B2 for split depression, and B3 for depression with multiple fragments. AO/OTA type C fractures involve the whole joint surface, with C1 being a simple split going through the metaphysis, C2 being an articular split with multiple fragments, and C3 having multiple fragments of the articular surface and metaphysis. The Ruedi-Allgower system (Figure 1-6) also subdivides the fractures into three types: type I is an intra-articular fracture without significant displacement, type II has significant displacement and minimal comminution, and type III has significant comminution as well as intra-articular displacement[26].

Both classification systems, AO/OTA and Ruedi-Allgower, stratify the range of severity effectively and have been deemed to have sufficient inter-observer reliability between major fracture types. However, at the subgroup level, both systems have exhibited poor inter-observer reliability in differentiating fracture severity[7].

Nonetheless, the opinion of an experienced traumatologist remains the gold standard for assessment of fracture severity against which any new objective measures must be gauged. The development of objective methods for assessing fracture severity would, however, enable greater inter-observer reliability and provide new opportunities for the field of orthopaedic research.

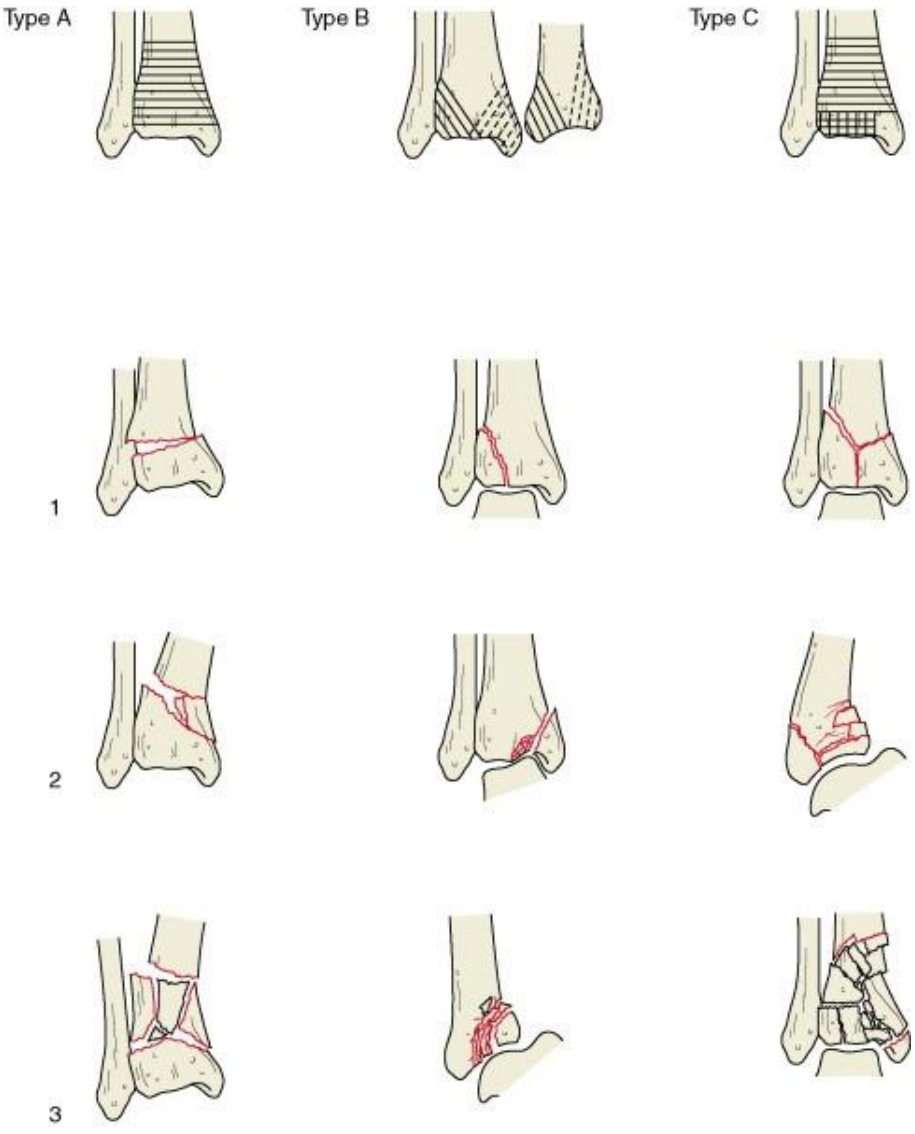

Figure 1-5: AO/OTA classification of plafond fractures.[33]

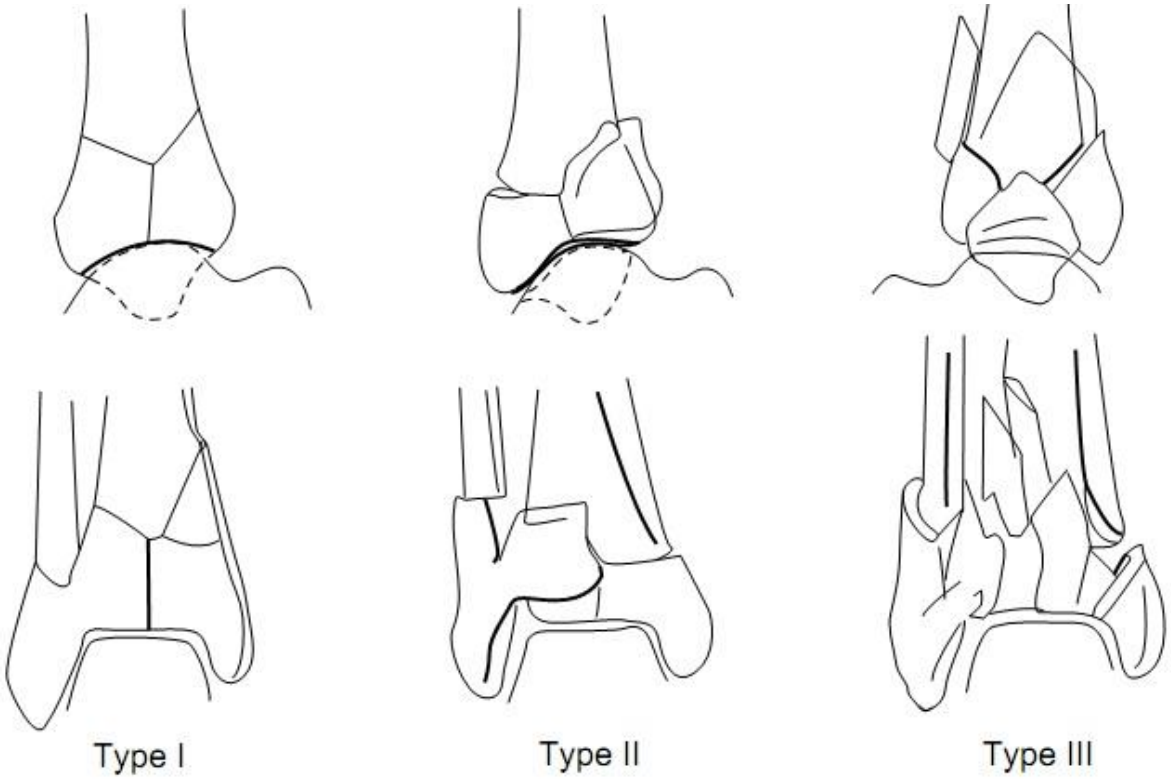

Figure 1-6: Ruedi-Allgower classification of tibial plafond fractures.[34]

1.4 The Calcaneus:

The calcaneus, or heel bone, is the largest bone in the foot and as such, is critical to normal foot function. It is capable of withstanding the high tensile, bending, and compressive forces experienced in daily life without fatiguing. The posterior half of the calcaneus constitutes the calcaneal tuberosity, a mostly cylindrical process upon which several strong tendons and ligaments attach. The anterior half of the calcaneus includes the cartilage-covered bony protuberances that comprise the subtalar and calcaneal-cuboid joints. The lateral-most aspect of the calcaneus forms the sinus tarsi. The distal-most end of the fibula extends in the lateral malleolus near this feature. The sustentaculum tali projects from the medial side of the calcaneus forming a shelf for the prominent middle facet [35].

The subtalar joint is the primary weight-bearing articulation of the calcaneus. It has three facets that articulate with the inferior talus: the anterior, middle, and posterior facets. The posterior facet is the largest and bears the majority of the subtalar joint loading. Together, the three facets allow for inversion and eversion of the foot. These motions are guided by substantial soft tissue structures surrounding the foot[36].

There are a number of critical soft tissues attached to the calcaneus. Notably, the Achilles tendon, the strongest tendon in the body, attaches the gastrocnemius, soleus, and plantaris muscles to the posterior aspect of the calcaneus. The calcaneal fibular ligament provides lateral stability to the foot and the posterior deltoid ligament provides medial support. Important to surgical reduction is the interosseous talocalcaneal ligament running just lateral to the sustentaculum tali through the canal. This strong ligament is

what makes the sustentaculum tali the “constant fragment” upon which surgeons base their reductions of fractured calcanei [35, 36].

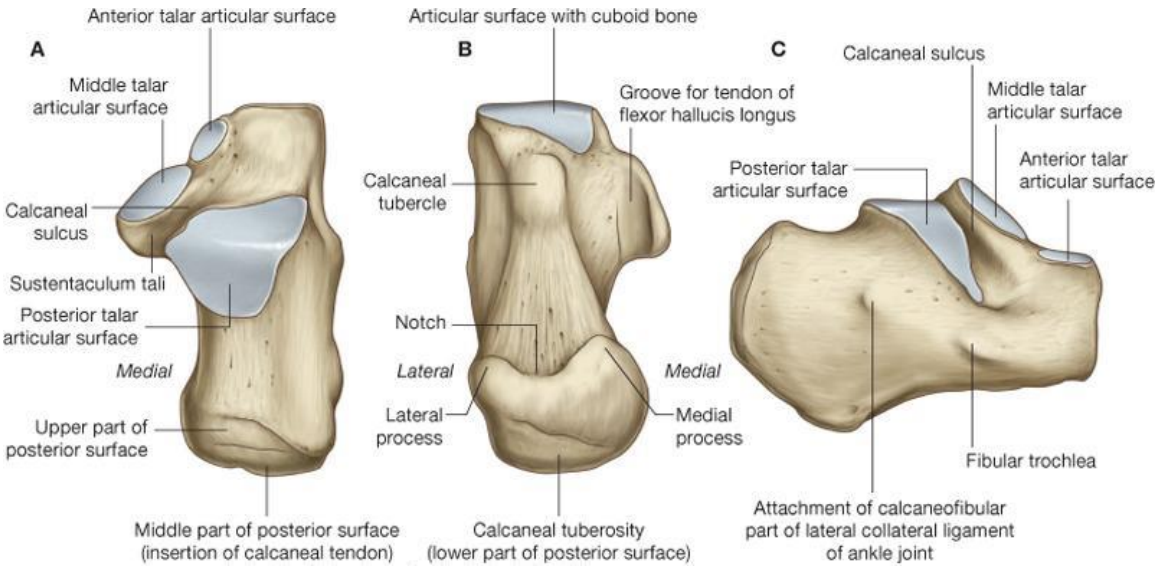

Figure 1-7: Anatomy of the calcaneus

1.4.1 Fractures of the Calcaneus

Fractures of the calcaneus constitute approximately 1-2% of all fractures; the calcaneus, however, is the most frequently fractured of the foot bones [37]. Calcaneal fractures can be minor injuries, but many are more severe, resulting from high energy mechanisms of injury like motor vehicle collisions and mechanical falls [38]. These high energy injuries often result in long healing times (up to two years) and eventual subtalar joint PTOA. Clinically, the Sanders classification system is the most commonly used for categorizing intra-articular calcaneal fractures. The Sanders classification consists of four primary types: type I – non-displaced fractures (less than 2mm displacement), type II – fractures consisting of a single intra-articular fracture dividing the posterior facet into two pieces, type III – fractures consisting of two intra-articular fractures dividing the posterior facet into three pieces, and type IV – fractures consisting of three or more intra-articular fractures. Subtypes for type II and III class fractures are defined as A for those involving the anterior calcaneus, B for those involving the middle of the calcaneus, and C, for those involving the posterior calcaneus [38-40].

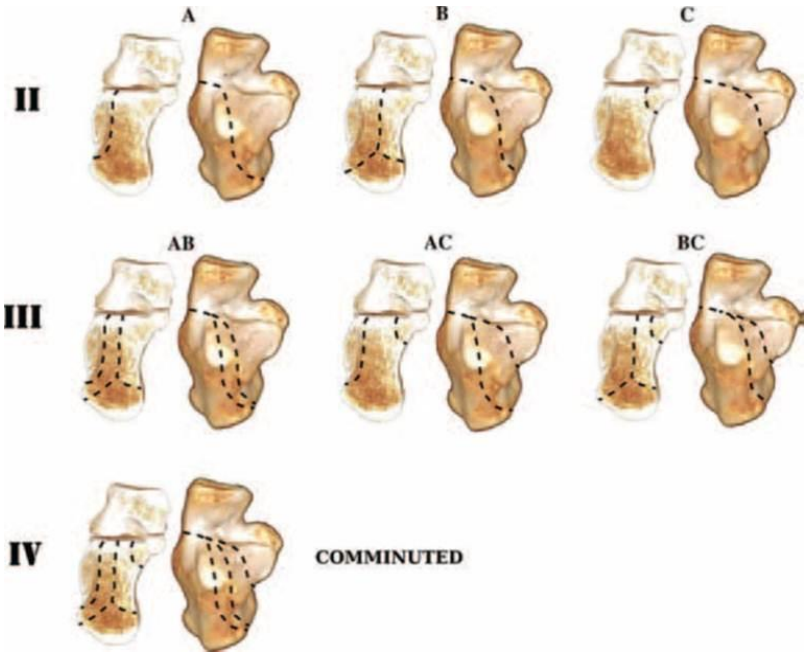

Figure 1-8: Sanders classification system for calcaneal fractures.[2]

Clinical management of these fractures involves choosing between three general treatment options: non-operative, open reduction with internal fixation, and percutaneous reduction and fixation. Non-operative care typically consists of elevation, application of ice, utilization of a splint, and early mobilization. Non-operative techniques reduce the risk of infection and other complications associated with surgery but can result in poor restoration of subtalar joint and hind-foot deformities that increase risk of PTOA development. Open reduction with internal fixation aims to restore joint congruity as accurately as possibly by directly visualizing the fracture. While this is generally considered to be the standard for reduction of the articular surface, the large wound created by the incision can be prone to infection and related complications. Percutaneous reduction techniques utilize CT scans to plan surgical approaches and provide fixation through minimally invasive incisions. The goal of this technique is to

restore articular congruity to the extent possible without the large incisions associated with ORIF techniques. At present, there is a paucity of evidence to definitively support the effectiveness of any of these techniques for all but the most severe of fractures [38].

1.5 Previous Fracture Severity Work

Acute fracture severity is considered one of the most important predictors of injury prognosis and risk of poor outcomes [10, 16]. Clinicians have utilized plain radiographs and CT to broadly classify fractures based on their locations and the relative number of fragments, but they have as yet been unable to reliably and objectively quantify severity [4, 7]. To address these problems, previous work developed an objective CT-based fracture severity metric that is capable of predicting PTOA. The original methods for obtaining fracture energy were robust but slow. Further work on an expedited objective methodology for assessing severity without directly quantifying fracture energy succeeded in reducing the time to evaluate cases from 8-10 hours down to under 15 minutes [11]. This was an important development as it moved the time required to obtain the objective metric into a clinically relevant time scale. Having the time to process a case on a clinically relevant time scale, typically under an hour, is important as it enables data to be given to the clinician while initial and definitive treatment options are being explored.

The basis of all objective fracture severity assessments is in the widely held belief among orthopaedic traumatologists that "the extent of bone, cartilage, and soft tissue damage is directly related to the energy imparted on these structures [4]." In 2002, Beardsley et al. showed that fracture mechanics theory for a brittle solid postulating a monotonic relationship between fracture surface area generation and energy absorption

could be applied to bone [41]. Utilizing CT data from fractures, the fracture surface area of bones could be discriminated and thus, the fracture energy measured. From these developments, a metric for quantifying the severity of tibial plafond injuries was developed showing excellent correlation with physician assessment of injury[5, 6, 10, 41]. To create this initial metric, important assumptions were made in the calculation of fracture energy. A number of these assumptions also apply in the context of this thesis.

One of the primary motivations for creating an assessment of severity is the determination of prognosis, in this case, the likelihood of PTOA development [10]. To more accurately predict PTOA, previously developed metrics have discounted fibular fractures to better estimate the amount of energy insult the cartilage experienced during the fracture. These assumed that any energy going through the fibula had circumvented the articular cartilage and, therefore, would not contribute to the development of PTOA[42]. Additionally, these metrics draw from the foundational fracture mechanics theory in their assumption that the material must be a brittle solid for the energy creating the fracture to have a monotonic relationship with the fracture liberated surface area. Therefore, at the high rates of loading experienced in fracture generation, bone was appropriately assumed to be a brittle solid. The reason for this relationship stems from the fact that the only way in which mechanical energy can be absorbed by these brittle solids is via the process of fracturing. These fractures create new surface area along the fractured edges; in an ideally brittle solid, this liberated surface area is directly proportional to the quantity of energy absorbed.

Ergo, a key factor in the creation of an objective fracture severity metric is the ability to measure fracture liberated surface area. In past studies, this liberated surface

area was quantified by utilizing an edge detection algorithm that found bone surfaces (edges) within two dimensional CT slice reconstructions [10, 11]. This identification of "free" bone surfaces was done without regard for whether the surface was native (i.e., existed prior to the fracture) or was inter-fragmentary (i.e., de novo bone surface liberated as part of the fracture). The bone surfaces were found both for the fractured limb and for the unfractured (intact) contralateral bone. The fracture liberated surface area was then identified by subtracting the surface area of the intact contralateral bone from the total bone surface area of the fractured limb slice by slice in the CT-image [4]. A significant amount of time (on the order of 8 to 10 hours per case) was required for completing the necessary manual interventions during this segmentation task. Therefore, while robust in the sense that manual verification of the segmentations was integral to the approach, this method had the distinct disadvantages of requiring the acquisition of an intact contralateral CT scan with which to compare surface areas and being extremely labor intensive.

Fracture energy calculations also need to account for variation in bone density, because the energy required to fracture the bone is greater for more dense bone. Following segmentation, the bone density was determined using the mean CT (Hounsfield Unit) intensities in semi-automatically identified cancellous, thin cortical, and thick cortical regions. Fracture energy calculations in this case were performed by multiplying the identified fracture liberated (de novo) surface area by the location and patient specific energy release rates for bone. One substantial improvement made upon this method is in the more robust and accurate localization of Hounsfield Unit dependent energy release rates. The method proposed in this thesis assigns the energy release rates

at each vertex along the de novo fractured bone surface rather than relying upon averaged values applied to the entire surface.

An expedited method was proposed in subsequent work to remove the requirement of an intact contralateral limb and to mitigate time consuming manual editing. The stated purpose for these changes was to make a metric specifically suitable for clinical application. Removing the requirement for an intact contralateral scan still required an intact limb surrogate, but allowed for expediting of the assessment process to clinically relevant time-scales (~15 minutes per case) and increased the clinical utility of the fracture severity metric. However, this work did not calculate fracture energy directly, instead focusing on more abstruse predictive metrics. These expedited methods were based upon identification and normalization of the quantity of de novo fracture area in relation to bone density. Fragment dispersion and articular comminution were also incorporated in the analysis.

The focus of the present work was to expand these prior efforts in objectively evaluating fracture severity by calculating fracture energy in any articular joint. In contrast to the prior objective severity assessments, this method for calculating fracture energy aimed to maintain the speed of the expedited metric, by minimizing manual intervention, and to expand the clinical utility of the method to allow for use on any articular joint, by not requiring the use of an intact contralateral or intact surrogate.

1.6 Rationale for Expanded Severity Metric:

Previous work successfully demonstrated that objective fracture severity metrics are an excellent tool for assessing injury severity in the plafond. Specifically, the fracture energy calculation showed strong predictive capabilities for the development of PTOA at a time of two years following the surgical treatment. These metrics have the potential to be integrated into the clinical setting to help guide a surgeon's approach to an injury. As previously discussed, there has also been promising work on development of an objective severity metric that can be obtained on clinically relevant time scales. This expedited assessment methodology, however, did not directly evaluate the fracture energy, but instead relied on more abstract indicators of injury severity.

The largest limitations for these extant fracture energy metrics has been the requirement either of a CT of the intact contralateral bone for the fracture energy calculation or the assumption of an anthropometrically scaled "normal" tibia and their singular study of the same 20 tibial plafond cases. These relatively restrictive requirements limited the clinical utility of the method to a single joint and necessitated the attaining of an intact contralateral CT scan or of additional anthropometric data. The fracture energy computation proposed in this paper aims to solve these problems and thereby increase the clinical and practical utility of an objective fracture energy metric. The methods developed are detailed, as is the application of these methods to assess fracture severity in a variety of joints.

CHAPTER 2: METHODS

The motivation for creating a new means for obtaining an objective fracture severity metric stems from the need to improve upon current fracture classification schemes used clinically. Where prior methods have yet to be used for joints other than the ankle, the methods developed and described herein are intended to be more broadly applicable. The methods build upon the foundations of these previous methods by generating an accurate estimate of fracture energy based solely on CT scans of the fractured bone. No intact contralateral or surrogate representation of an intact limb is required. Through the use of an automated trained classification system designed for identifying bone surfaces as either native or de novo, fractured surface area can be directly determined in a 3d working environment. This advance facilitates the study of a larger number of cases and supports application of the severity metric in joints other than the tibial plafond.

The research performed in this study involved both clinical and computational components. Orthopaedic surgeons at the University of Iowa Hospitals and Clinics, the University of Indiana, and the University of Utah performed the clinical work in collaboration with the author. The computational components of the work were performed by the author or under his direct supervision, building upon previous research conducted in the Orthopaedic Biomechanics Laboratory at the University of Iowa.

2.1 Segmentation and Model Creation:

The fracture energy calculation is based upon 3d surface models of fractured bone identified and segmented from CT scan data. Segmentations were first performed using purpose-written MATLAB code originally developed by Thaddeus Thomas Ph.D., Andrew Kern M.S., and Donald D. Anderson Ph.D. to automatically identify and separate fracture fragments with minimal user intervention. From these segmentations, 3d models were produced and analyzed to identify new surfaces of the bone liberated in the fracturing process. This process relied heavily upon a surface classification algorithm trained to recognize different surfaces based upon geometric and image intensity features. However, the segmentation task itself remains the most labor-intensive component of objective fracture severity analysis.

Differentiation of human bone from surrounding soft tissues within CT images is a challenging task. In CT imaging, normal cortical bone is easily discerned from surrounding muscle, fascia, and other soft tissues. However, cancellous bone is relatively less dense as a consequence of its porous trabecular nature. This can lead to cancellous bone having similar attenuation values to its surrounding soft tissues. When cortical bone is intact, cancellous bone is easily identified, as it is completely bounded by the denser cortical shell. However, when the cortical shell is fractured it can become difficult to discriminate between the soft tissue and the cancellous bone due to similar attenuation values. This is the primary need for user intervention and the limiting factor in decreasing the segmentation time.

Once bone/bone fragments were segmented from the CT scans in the purpose-written MATLAB code, the scans were loaded as NIFTI files into ITK-SNAP. This step was performed to correct any minor errors and inconsistencies remaining in the segmentation as a result of the inherent difficulties described above in performing an automated segmentation. After these corrections were completed, ITK-SNAP was utilized to export all fragments as individual STL models, the 3d model format used later in the de novo fractured bone area measurement. The STL models were then imported into Geomagic for a semi-automated smoothing and decimation routine to attain a more accurate representation of the bony surface and prepare it for subsequent fracture severity computation. Each properly prepared STL surface file of a fracture fragment was then saved to be imported into the MATLAB bone surface classification algorithm (Figure 2-1).

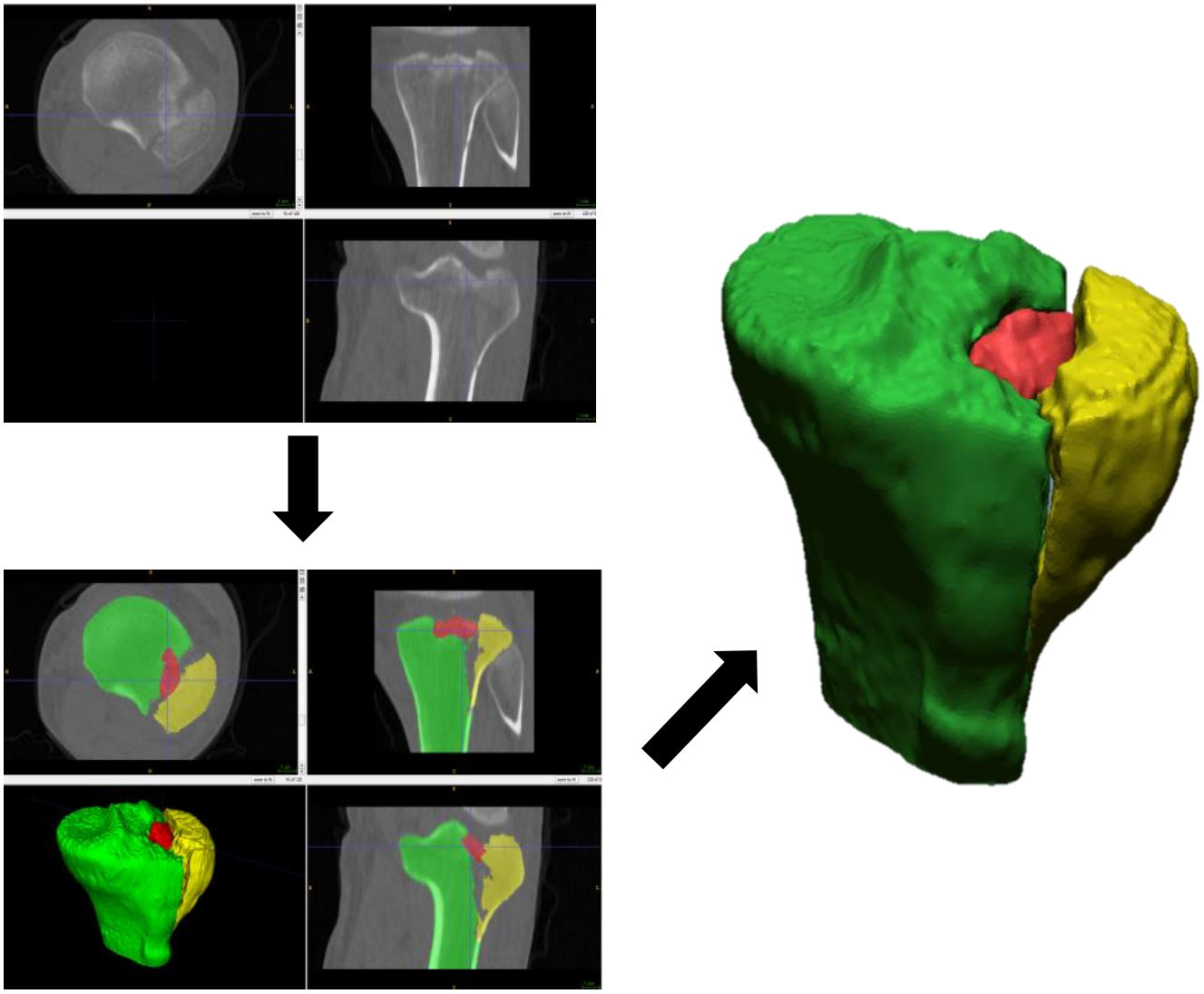

Figure 1-1. Workflow for fragment model creation from CT scan to segmented model to smoothed and decimated surface.

2.2 Classification:

The classification of separate bone surfaces was performed to distinguish intact and fractured bone for use in the severity analysis. Initial sets of fractured bone fragments in which the intact and fractured surfaces had been painstakingly manually identified were utilized to train a classifier leveraging the MATLAB function 'predict'. This function offers a number of different machine learning classification strategies and options. For present purposes, a Naïve Bayesian Classifier was trained. This is a simple technique for discriminating between classes. It assumes that each feature used to differentiate between classes is independently predictive of the probability it will have a specific classification. Specifically, this is implemented through the following formulation to minimize the expected classification cost:

$$\hat{y} = \arg\min \sum_{k=1}^{K} \hat{P}(k|x)C(y|k)$$

Where $\hat{y}$ is the predicted classification, K is the number of classes, $\hat{P}$ is the posterior probability of class k for observation x, and $C(y|k)$ is the cost of classifying an observation as y when its true class is k.[43-45]

There were eight features selected for use in the naïve Bayesian classifier chosen based on their ability to best delineate fractured surface area. There were 6 image intensity based features and 2 geometrically based features. The image intensity based features included the CT Hounsfield units, the image sheetness, and variations of the two at different depths. The image sheetness is a second derivative image capable of detecting both direction and magnitude of edges shown in Figure 2-2 as contrasted

against its original CT data. Obtaining the CT Hounsfield unit values from the STL models was accomplished using the mean of the normal vectors on each face attached at a vertex for all vertices. The normals of the STL models generated in the segmentation process were projected into the CT image at 5 depths ranging from 0mm to 2mm at 0.5mm intervals from the vertex as shown in figure 2-2. The Hounsfield Unit intensities at the nearest voxels were interpolated for use in classification. The mean, standard deviation, and difference in HU between the 0mm and 2mm depths were computed on both the CT and sheetness images and comprised the 6 image intensity based classification features.

The two geometrically based classification features were obtained from STL models' vertices without relation to the image based intensity information. This is analogous to how the prior fracture energy metric had identified fractured regions with the exception of now being computed in three dimensional space. The minimum, maximum, and gaussian surface curvatures, exemplified in Figure 2-3, at each vertex were computed for use in training the classifier [46, 47]. The maximum and gaussian curvatures were directly included in the training of the classifier while the minimum curvature was indirectly included as it was required for computation of the gaussian curvature. These curvatures were included to help the classifier better detect fractured regions as intact bone regions tend to have lower curvature and fractured bone tend to have higher curvature.

0mm	0.5mm	1.0mm	1.5mm	2.0mm
700HU	650HU	625HU	400HU	400HU

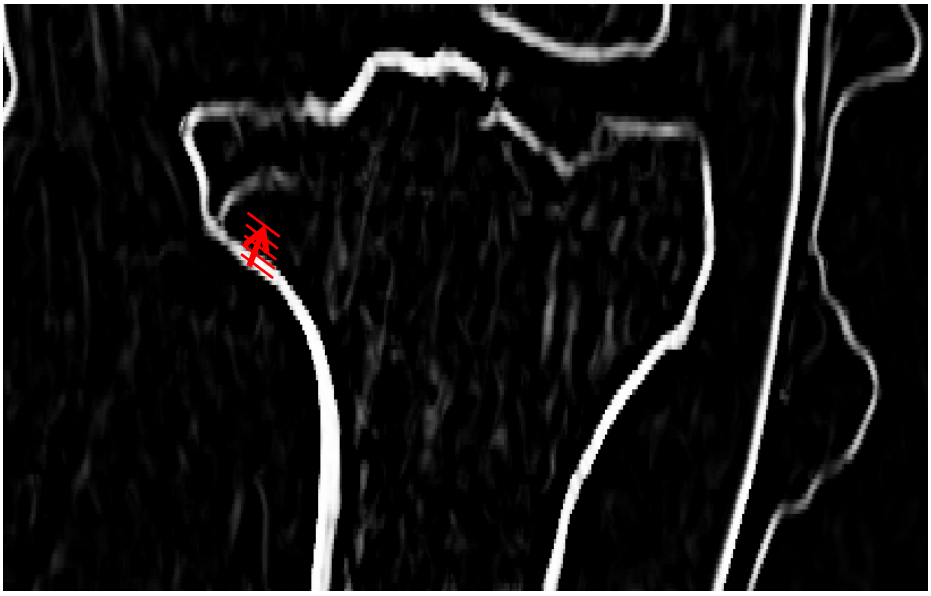

Figure 2-2: Comparison of CT (top) and Sheetness (bottom) images at 5 depths between 0 and 2mmalong the vertex normal as shown by the arrow and lines on each graph.

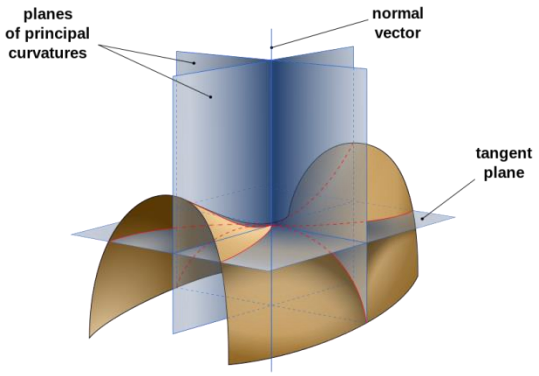

Gaussian curvature is computed using the normal vector to define normal planes to the surface then identifying the intersection of the surface with the planes and multiplying the minimum and maximum curvature at that location.

Figure 2-3: Gaussian Curvature Definition[1].

These features were then passed to the classifier which, based on the 3 training data cases, computed the probability each vertex had of being fractured or intact. If the probability of being fractured was greater than 0.5, then the vertex would be classified as fractured. A flowchart demonstrating the classifier logic is shown in Figure 2-4. The generation of fractured vertex probability is based upon the equation described earlier in this chapter. Each vertex feature is assumed to be independent from the other features and therefore, each contributes independently to the probability the surface will be classified as fractured. This probability is based upon the likelihood the vertex would be classified as fractured with a given value of a feature in the set of training data. After predictions were made, data was displayed in the 3d interface. In this interface, faces were classified as fractured if they contained 2 or more vertices identified as being in the fractured region. Manual editing of the classification was then enabled on each fracture fragment.

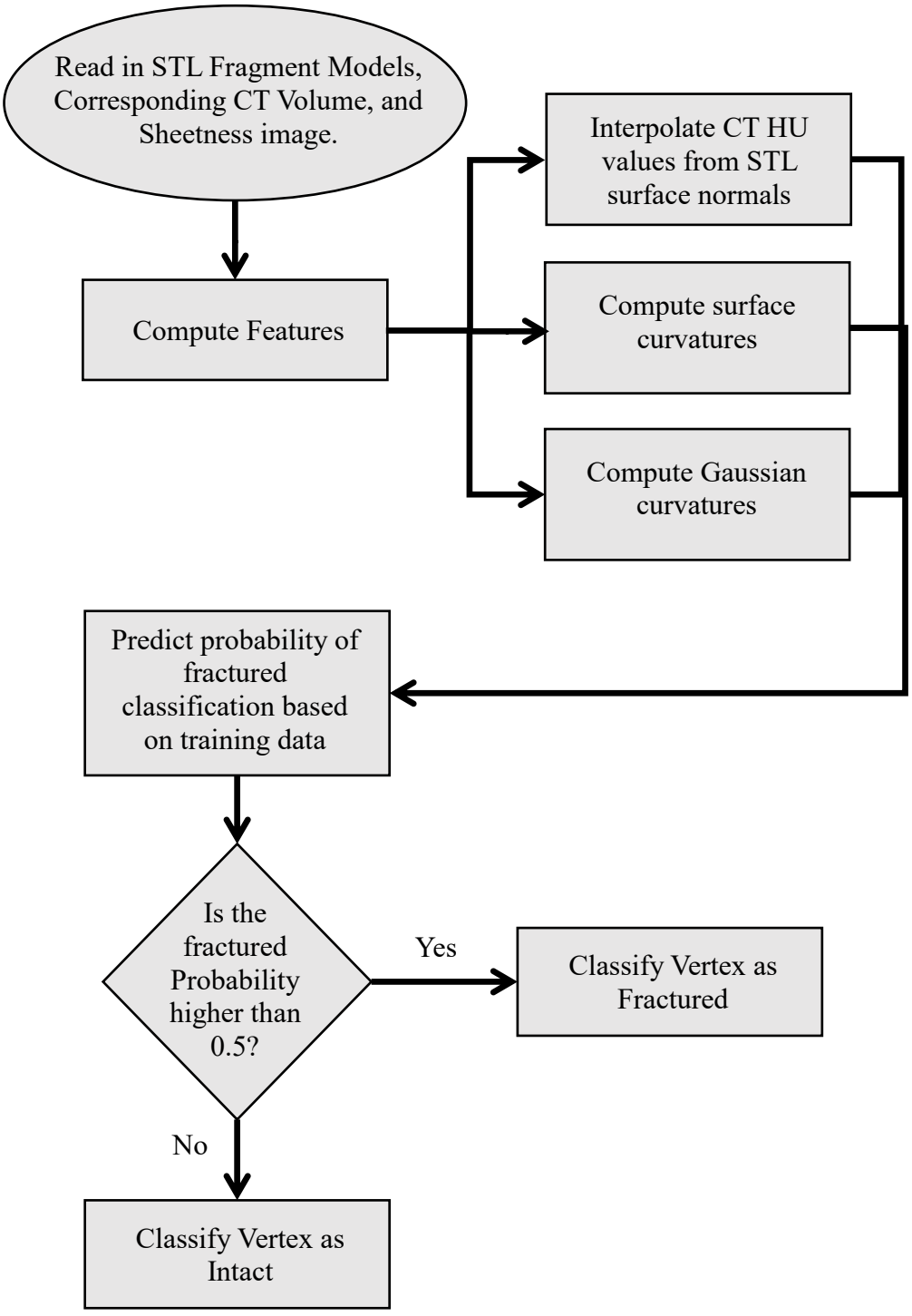

Figure 2-4: Logic of Naïve Bayesian Classifier applied to predict de novo fractured bone area.

After the probability of each vertex being classified as fractured or intact is computed, identification of the fractured surface area is not complete. If only the classifications based upon the Naïve Bayesian Classifier were used, the surface would be divided into heterogeneous regions with improperly classified vertices scattered throughout. In order to achieve homogenous fractured and intact regions, a graph cut algorithm was used to separate the regions on each fragment (as shown in Figure 2-5). A minimum-cut/maximum-flow (min-cut/max-flow) algorithm was implemented to create the cut. The minimum cut is defined as the cut that has the lowest edge cost. Edge costs, used in the building of this tree, are defined from the predicted classification probabilities and the surface curvatures (normalized between 0 and 1).

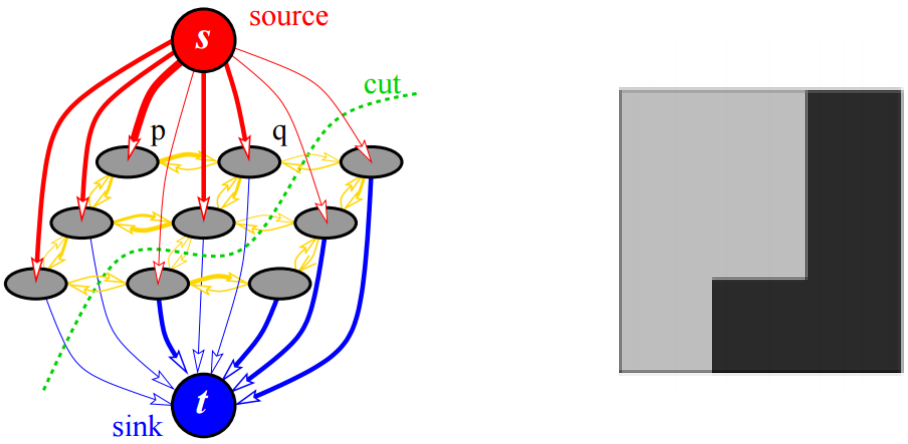

Figure 2-5: Left - An example of a graph cut separating two regions is shown here by the green dotted line. Edge costs are reflected by their line thickness. Right – regions as separated by the cut shown[48].

After the graph cut was used to nominally define the intact and fractured regions, any spurious region classifications were corrected through a 3d user interface. The STL model of each individual fracture fragment was isolated and viewed independently of the other fragments to allow for errors in the classification to be corrected. An example of a small typical error in the classification can be seen in Figure 2-6 for illustrative purposes. Errors in the classification typically occur in the cortical bone in areas of relatively high curvature. The area circled shows such an error in the classification of the right-most fragment in the model. The fragment is selected (shown highlighted in red on top left and middle left) and viewed independently (middle) in order to correct the classification. All fragments were visually inspected to ensure that the classifier had correctly identified fractured and intact regions of bone. This process can be repeated as many times as necessary on each fracture fragment until the classifications are deemed to be correct.

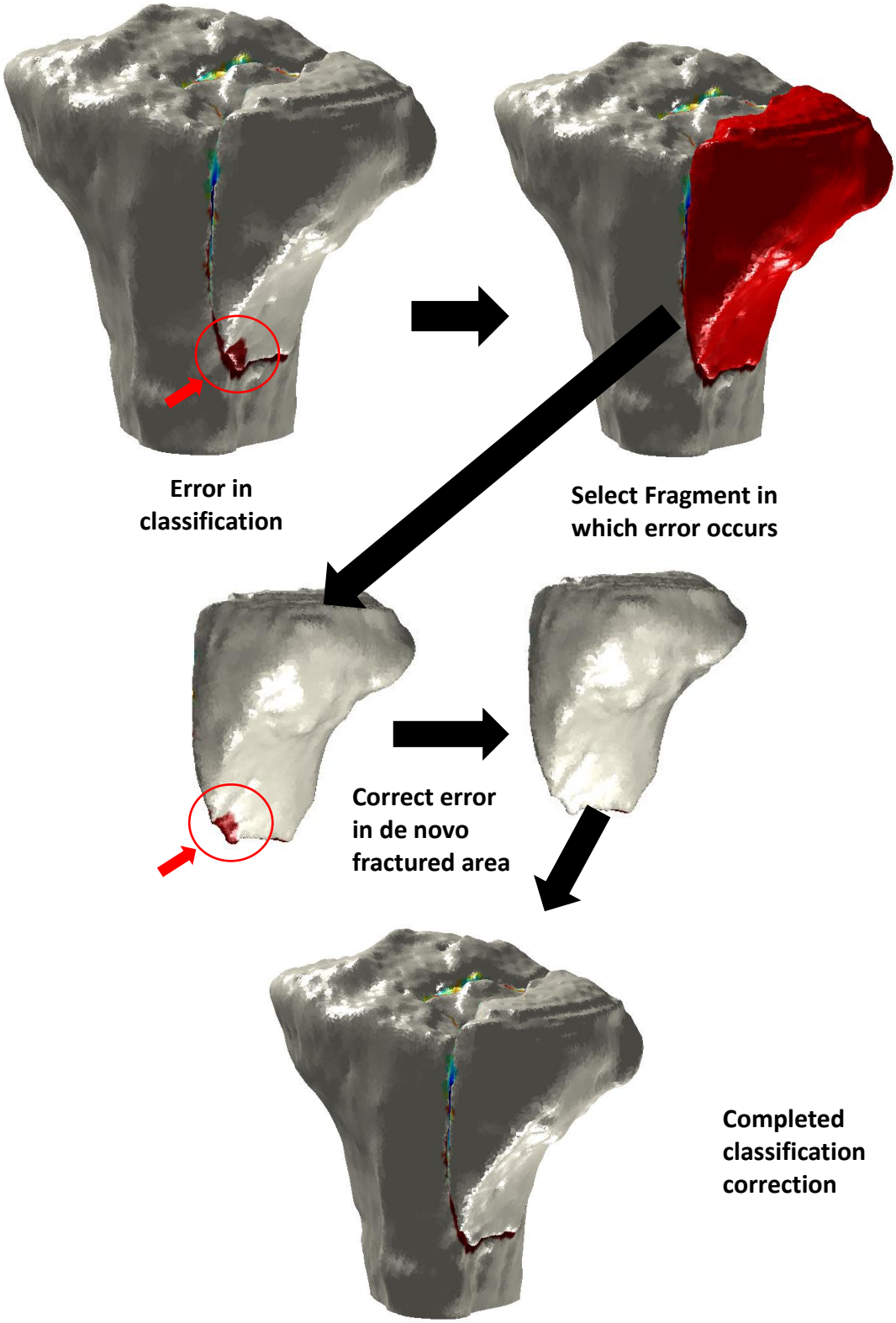

Figure 2-6: Classification Correction Work Flow

2.3 Severity Computation:

The fracture-liberated surfaces were then utilized to estimate the energy of the fracture. All faces of the bone fragment models with 2 or more vertices classified as fractured were included in the fracture area computation. The closest CT Hounsfield Unit (HU) intensity was then determined at the 3 vertices and averaged to obtain an approximation of the bone density at that area. The fracture energy was then determined using the following equation:

$$\boldsymbol{Energy(J)} = \frac{1}{2} * [SA_{liberated}(m^2)] * \left[\left(\frac{HU}{10^{2.87}}\right)^{\left(\frac{1}{1.45}\right)} \left(\frac{g}{m^3}\right)\right] * \left[\left(\frac{12000}{1.98}\right)\left(\frac{J * m}{g}\right)\right]$$

Where: the first bracketed term, SA, is the surface area scaled by ½ in order to account for only the new surface area generated along the cut plane of the fracture and not both sides of the cut plane on each fracture fragment as is segmented; the second bracketed term represents the density based upon the CT Hounsfield Unit intensity, shown in the equation as HU as determined by Snyder et. al. in 1991;and the third term is the density dependent energy scaling factor empirically determined in prior work by Beardsley and implemented in this form by Thomas[3, 10, 41, 49, 50]. Figure 2-3 demonstrates the classification of surface area into intact and fractured bone. The colored region shows the de novo fracture liberated surface area with the densities shown. In essence, this provides an idea of where the energy was released from in the fractured bone as higher density bone is associated with higher fracture energy through the equation above. The density is calculated in the second portion of the equation from the CT Hounsfield Unit intensity in grams/meter^3.[3, 49]. This density is then scaled by an empirically derived energy release

rate for human bone. This energy release rate is the same across all cases analyzed and does not account for patient factors such as age or gender. This is a limitation of the study as it is known that bone will have different mechanical properties depending upon patient factors. However, in prior work it was established that these differences were relatively minor in the context of the articular fractures being studied.

Another limitation is that acquisition-specific CT-parameters were not accounted for in the calculations. There are numerous CT-parameters that might affect the results on a case to case basis. The first is the voxel size. Smaller voxels offer better resolution and therefore, the potential for more accurate discrimination of the fractured area. Larger voxels affording poorer resolution are then more prone to less accurately identified fractured area. This difference was accounted for in the data selection process. Only scans with all voxel dimensions less than 1mm were evaluated. Fortunately, modern CT acquisition protocols for articular fractures routinely deliver spatial resolutions in this range. Any error in the boundaries of the fractured area due to the voxel sizes is likely to be random and therefore averaged out. Another problem with large voxel sizes is partial volume effects. This occurs when the voxel is too large to capture the details smaller than the voxel size itself. For example, in this study, voxels along the fracture edge are likely to only be partially filled with fractured bone. Since the Hounsfield unit value of the voxel is the averaged intensity of the less dense water and the more dense bone, the fractured edge may appear less dense than reality. To account for this factor, the Hounsfield units were sampled 3 voxels in along the surface normal along the fracture boundary.

The other acquisition specific CT-parameter that has bearing on the fracture energy calculation is the convolution kernel used to reconstruct the image. Convolution kernels are designed with one of two primary purposes: to create an image to improve discrimination of bony edges or to improve ability to detect low contrast soft tissue structures. The images created from kernels used for bony edge detection are susceptible to pixel noise appearing grainy while soft tissue kernel images appear smooth and lack highly defined bony edges. To account for these differences, an anisotropic diffusion filter is applied during segmentation to enhance bony edges and smooth pixel noise for accurate model creation. As this filter changes the image HU intensity values and could affect outcomes, the original CT scan acquisitions are used after the segmentation step to be sampled in severity computation.

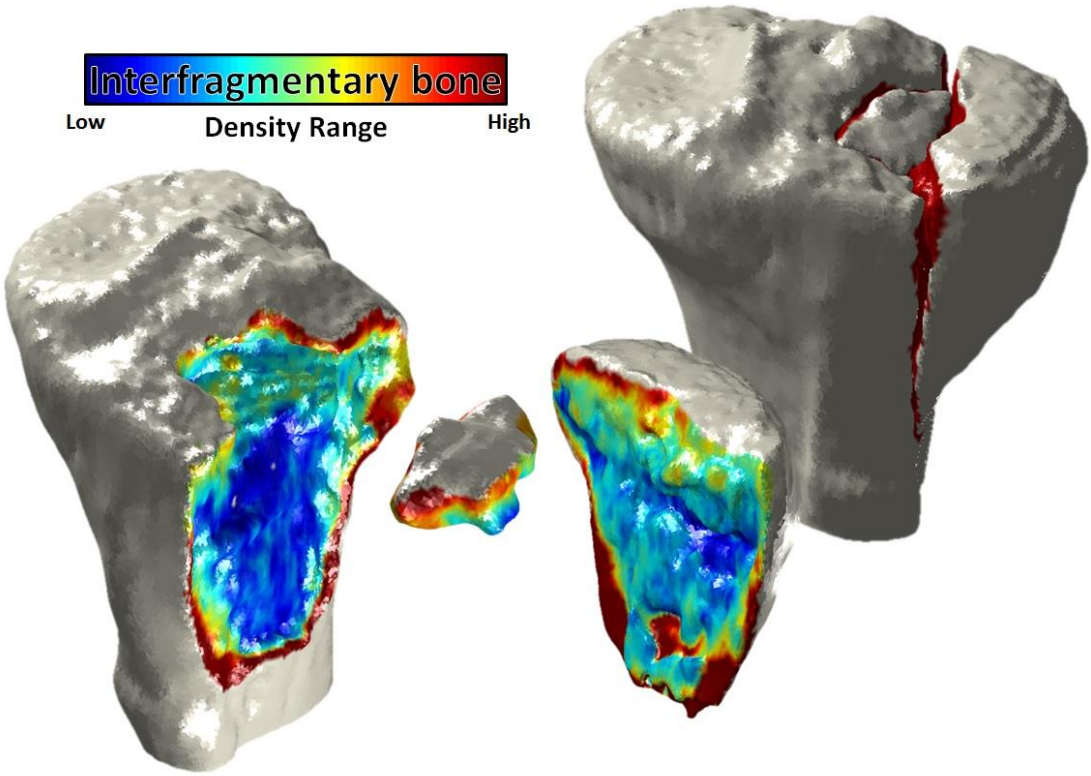

Figure 2-7. The fracture-liberated surface area and bone density values used to calculate fracture energy.

2.4 Clinical Data Gathering:

The initial 20 tibial plafond fracture cases that were the focus of prior development work had been obtained under an NIH-funded grant investigating PTOA. These prior cases, for which previously validated methods had been used to measure fracture energy, were used for validation of the present method. Additional fracture cases were provided under grants from the NIH and the Foundation for Orthopaedic Trauma, in collaboration with the University of Indiana and the University of Utah.

2.5 Plateau Rank Ordering:

In collaboration with the University of Indiana, a comparison of the computed fracture energies and surgeon assessment of fracture severity for 20 tibial plateau cases was performed. The 20 cases were selected by a fellowship-trained orthopaedic trauma surgeon to fully span the spectrum of fracture severity. The cases to be rank ordered by severity were taken from a larger series of 50 tibial plateau fractures by a fellowship-trained orthopaedic traumatologist. Fracture classifications ranged from OTA 41-B3 to 41-C3.[26] IRB approval was obtained from both institutions. Patients included in the study ranged in age from 18 to 70-years-old. There were 12 males and 8 females.

The purpose of this study was to determine the capability of an objective CT-based fracture energy metric to assess fracture severity by comparing it to the current gold standard; the subjective expert opinion of orthopaedic traumatologists. Assessment of expert opinion was done by rank ordering the cases.

The raters were given a PowerPoint with 20 slides corresponding to the 20 cases. Each slide contained an AP and lateral plain radiograph of the cases. The raters were asked to view the slides in the slide sorter view with occasional inspection of individual slides as needed. Figure 2-8 shows the PowerPoint format the surgeons were asked to use in ordering the cases. With the slide sorter view open, they were asked to order them based upon severity with the first slide being the least severe and the last slide being the least severe. They were asked to save the PowerPoints with their finalized ordering and

return them for use in the study.

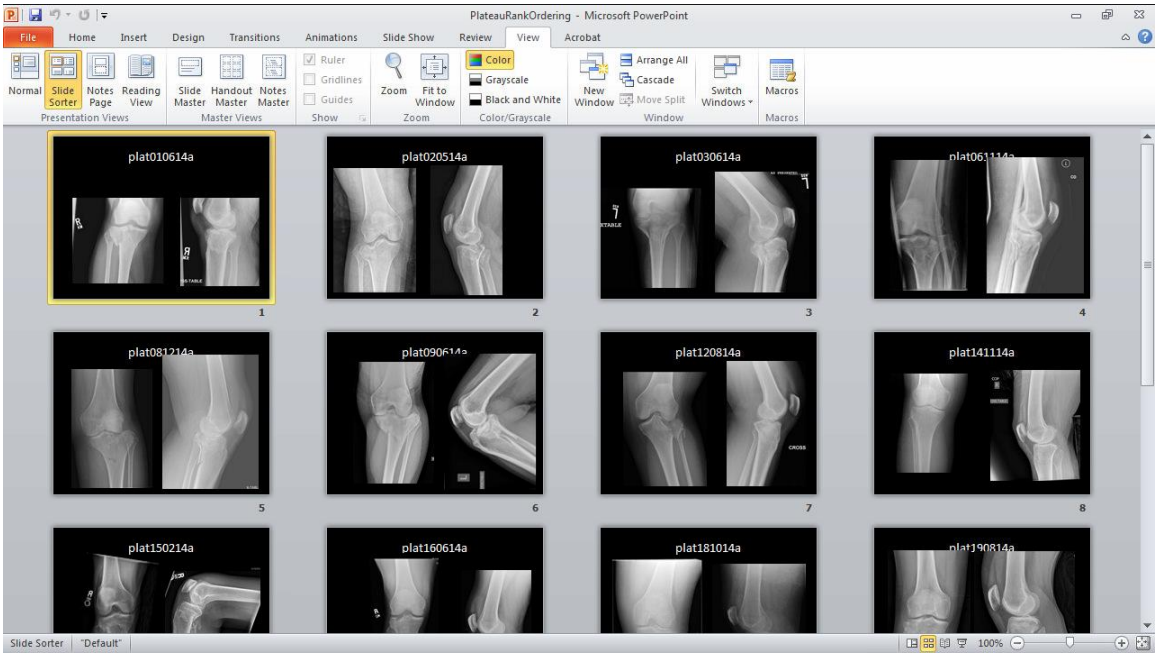

Figure 2-8: PowerPoint format used for ordering plateau fracture cases.

Similarly, the fracture energy for each case was determined and the cases were rank ordered from lowest to highest energy. This ordering was then compared with the ordering of the expert raters. Concordance, a measure of agreement between rankings, between the raters and the fracture energy was then computed.

2.6 Concordance:

Concordance is a statistical method with which the probability of two cases having the same ordinal ranking by two different raters or methods can be measured. Concordance is determined by taking the number of concordant pairs of ratings divided by the total number of possible pairings. A pair of ratings is deemed concordant if cases with higher rankings by one rater or metric are also ranked higher by a second. A perfectly random assignment of rankings between two reviewers would then produce a

concordance of 0.5, as any case pairing would have a 50% chance of being concordant. This method was utilized in all studies where comparisons of ranking and/or classification were evaluated.

Ranking Position	Rater 1:	Rater 2:
1	A	A
2	B	B
3	C	D
4	D	E
5	E	C

Concordance is found by taking all possible pairs of ratings that occur at the same position between raters and calculating the number of concordant pairs divided by the total number of pairs. If there is a tie between ratings in a pair (as there often is when rating using a finite classification system), then it is counted as having half of the value of a truly concordant pair. Simply put, if the sign (i.e. >,<) of the pairs are the same, then the pairs are concordant.

Position Ranking Comparison	Rater 1 Ranking	Rater 2 Ranking	Concordant pair (1 for concordant, 0.5 for ties and 0 for non-concordant)	Total pairs
Position 1 vs 2	**A < B**	**A < B**	**1**	1
Position 1 vs 3	**A < C**	**A < D**	**1**	2
Position 1 vs 4	**A < D**	**A < E**	**1**	3
Position 1 vs 5	**A < E**	**A < C**	**1**	4
Position 2 vs 3	**B < C**	**B < D**	**1**	5
Position 2 vs 4	**B < D**	**B < E**	**1**	6
Position 2 vs 5	**B < E**	**B < C**	**1**	7
Position 3 vs 4	**C < D**	**D < E**	**1**	8
Position 3 vs 5	**C < E**	**D > C**	**0**	9
Position 4 vs 5	**D < E**	**E > C**	**0**	10
		Total	**8**	10
		Concordance	**80%**	

The 80% concordance found here corresponds to a 80% chance that two cases will have the same ranking by rater 1 and rater 2.

Figure 2-9: Concordance calculation example

2.7 Schatzker Classification:

Performed in cooperation with the University of Utah, Schatzker classification of tibial plateau fracture was compared with fracture energy. A series of 40 patients with tibial plateau fractures were consented for the study. Standard of care pre-operative CT scans were obtained and used to clinically assess severity by classifying cases according to the Schatzker classification. The series contained a variety of plateau injuries ranging from Schatzker classification I to VI fractures as judged by expert surgeons at time of injury. The pre-operative CT scans were also segmented and used in determination of fracture energy. As fractures with higher Schatzker classifications are generally considered to be more severe, the classifications were used to rank the severity of the fractures. Accordingly, the fracture energy measure was also used to rank order the 40 cases. Concordance between the Schatzker classification ranking and fracture severity ranking was then used to characterize agreement in their assessments.

2.8 Calcaneal Fracture Energy:

IRB approval was obtained for eighteen patients with nineteen intra-articular calcaneal fractures seen at the University of Iowa Hospitals and Clinics. The patients were selected from a series of 120 cases presently being followed. Pre-operative CT scans were obtained for all patients in accordance with the standard of clinical care to assess severity. Clinically, the Sanders classification was evaluated by a fellowship-trained orthopaedic traumatologist for each fracture, utilizing the pre-operative CT scans. Four expert surgeons also evaluated the post-reduction articular step-off to consider as a potential confounder.

The pre-operative CT scans were segmented and processed as described in chapter 2.1 for use in the in the fracture energy metric. Both fracture energy and Sanders classification (described in chapter 1.4.1) were used to assess initial fracture severity. The fracture energy and Sanders classification were then evaluated against post-operative outcomes. The Kellgren Lawrence (KL) grading system, developed as a radiographic indicator of arthritis development, was used to evaluate patient outcomes at their last followup [51]. The KL grading system categorizes radiographically perceptible changes in OA severity into 5 grades. A KL grade 0 indicates a radiographically normal joint with no visible arthritis and a grade 4 indicates severe radiographically detectable development of arthritis. Grade 2 has been considered to be the threshold for PTOA appearance. This grading scale was then used to judge the predictive abilities of both the Sanders classification and fracture energy metric.

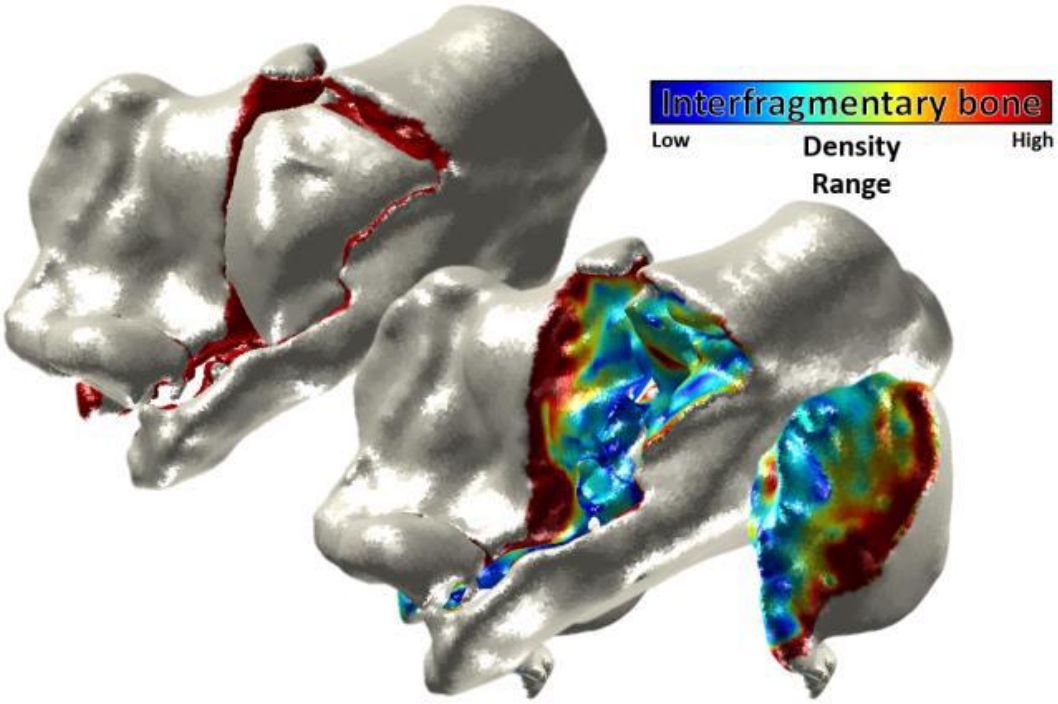

Figure 2-10. 3d model of a Sanders class III intra-articular calcaneal fracture. Left: inter-fragmentary surface area (red). Right: inter-fragmentary bone with bone density range.

2.9 Fracture Energy Comparison:

A combined effort between the University of Iowa, University of Indiana, and University of Utah hospitals has resulted in over 109 total fractures of the tibial plafond (31 cases), plateau (61 cases), and the calcaneus (17 cases) for study. The same, versatile fracture severity assessment methodology was shown to be capable of handling these 3 diverse injury types. This allowed an unprecedented direct objective comparison of injury severity between the three different types of fractures. The range of fracture energies in this study is expected to be similar across injuries with similar mechanisms.

CHAPTER 3: RESULTS

The fracture energy assessment methodology was applied to analyze 3 different joints in 2 different fractured bones; energy of fractures was determined in the tibia for the tibiofemoral (plateau) and tibiotalar (plafond) joints and in the calcaneus for the talo-calcaneal (subtalar) joint. Pre-operative CT scans were obtained for 61 plateau, 31 plafond, and 19 subtalar joint fractures from 3 institutions.

3.1 Fracture Energy Assessment

The fracture energy assessment used in this thesis was computed on all 111 cases studied. For these cases, the average time to segment and prepare models for the classifier as described in chapter 2.1 varied but took on the order of 30-45 minutes per case. The classification of de novo fractured area, detailed in chapter 2.2, for the cases was much faster; the classification took between 1 and 15 minutes depending upon the amount of classification correction performed. The calculation of fracture energy occurred after the classification and never required more than 1 minute to complete.

3.2 Fracture Energy Validation

The fracture energies computed using the new assessment methodology were compared against those computed using the prior method for validation purposes. The twenty tibial plafond cases previously analyzed were evaluated using the new methodology. A comparison between the results are shown in figure 3-1. There was a strong agreement between the previous fracture energy measure and the present fracture energy measure with an R^2 correlation of 0.9434. On average, there was a bias that the prior methodology measured around 1.5J higher than the present method; based upon

these cases, the data suggest that 95% of measurements with the new methodology will be within 3-5J of those made using the old method.

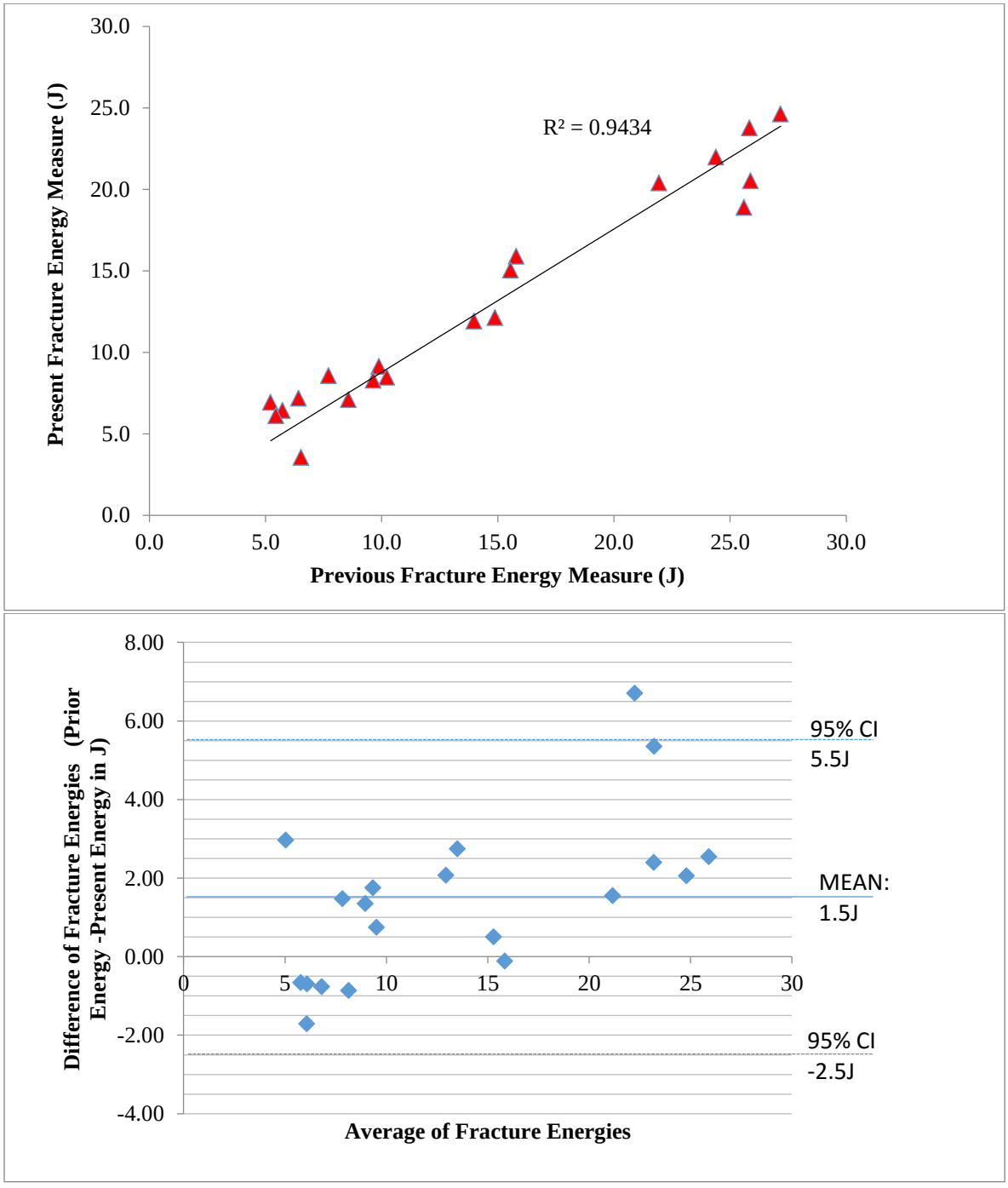

Figure 3-1: A comparison between the previously established fracture energy methodology and the present fracture energy method. Top: Graph of prior vs present energy methodologies. Bottom: Bland-Altman plot of prior vs present energy methodologies.

3.3 Plateau Rank Ordering:

The fracture energies computed in twenty tibial plateau fracture cases selected to span the injury severity spectrum ranged from 5.1 to 23.6 Joules (J). A high level of agreement was found between the six experienced orthopaedic trauma surgeons who completed the severity ranking. Concordances between the surgeons ranged from 82.1% to 92.6%, with a mean of 87.4%. The concordance between the surgeons and the fracture energy ranking of severity were slightly less high, ranging from 70.5% to 78.4%, with a mean of 74.7%.

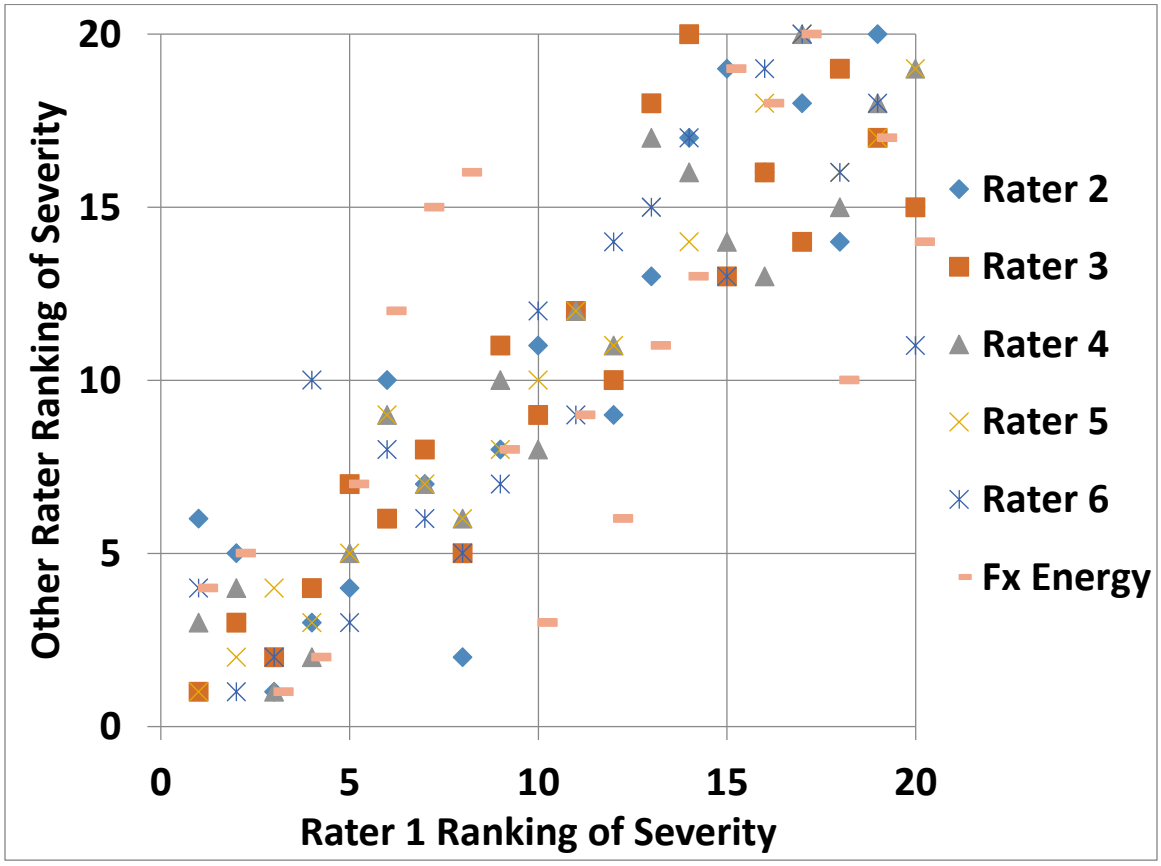

Figure 3-2: Rater 1 ranking of severity vs each individual ranking of the other raters.

Table 3-1: Concordance between six expert orthopaedic traumatologists and fracture energy

Rater	B	C	D	E	F	Fracture Energy
A	84.2%	87.4%	88.9%	92.6%	83.7%	**75.8%**
B		82.1%	86.8%	85.3%	84.7%	**76.8%**
C			86.8%	85.3%	81.6%	**70.5%**
D				92.1%	83.2%	**78.4%**
E					87.9%	**75.8%**
F						**71.1%**

3.4 Schatzker Classification:

The average fracture energy increased monotonically with increasing Schatzker classification. This indicates general agreement between the Schatzker classification and the energy involved in producing the fracture. Despite this general trend of agreement, the energies showed a significant degree of variance in some classes. Schatzker class II fractures, for example, had overlapping energy fractures with all other classes ranging from 3.2J to 17.7J fractures. This large degree of variance could easily explain outliers in previous studies that have utilized the Schatzker classification system as a surrogate measure of initial fracture severity.

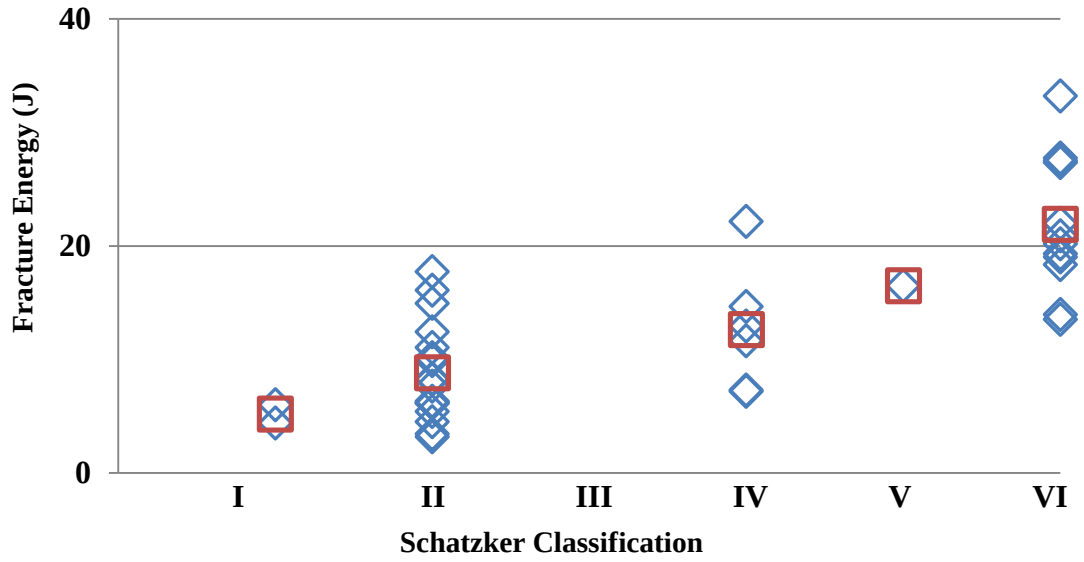

Figure 3-3: Schatzker Classification vs Fracture Energy with averages by classification (indicated by red boxes).

Table 3-2: Comparison of fracture energy and Schatzker Classification

Schatzker Class	Number of cases	Mean	Minimum	Maximum	Standard Deviation
I	2	5.2	4.4	6.0	0.8
II	19	8.8	3.2	17.7	7.3
III	0	N/A	N/A	N/A	N/A
IV	6	12.6	7.2	22.2	7.5
V	1	16.5	16.5	16.5	0.0
VI	12	21.9	13.5	33.2	9.8

3.5 Calcaneal Fractures:

There were 19 calcaneal fracture cases analyzed for severity. The fractures ranged in their nature from Sanders classification II to IV. The energy of the fractures ranged from 12.3J to 24.5J, with an average energy of 18.0±2.9J. Eleven cases were evaluated for PTOA development between 20 and 74 months post-operatively. A concordance of 75% was observed between the Sanders classification and the fracture energy measurements. There were more complex relationships observed between the KL grades, articular step-off, classification, and outcomes. Figure 3-4 demonstrates some of these relationships, with cases segregated based upon articular reduction quality. Figure 3-5 shows the relationship between fracture energy and Sanders classification, and figure 3-6 shows the relationship between Sanders classification and the KL-grade.

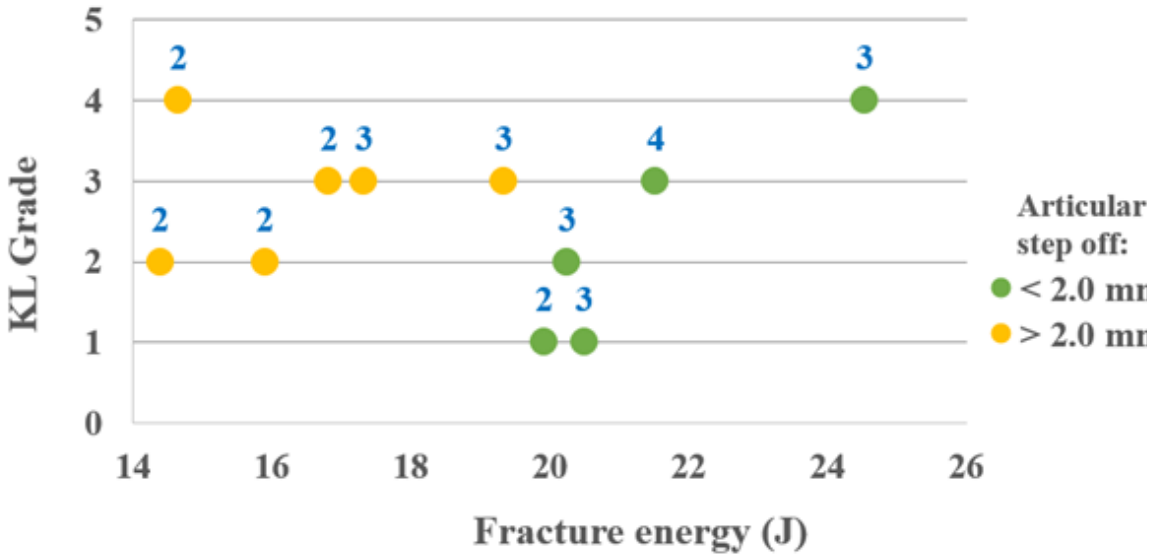

Figure 3-4: KL Grade vs Fracture Energy. Number above data points indicates Sanders classification.

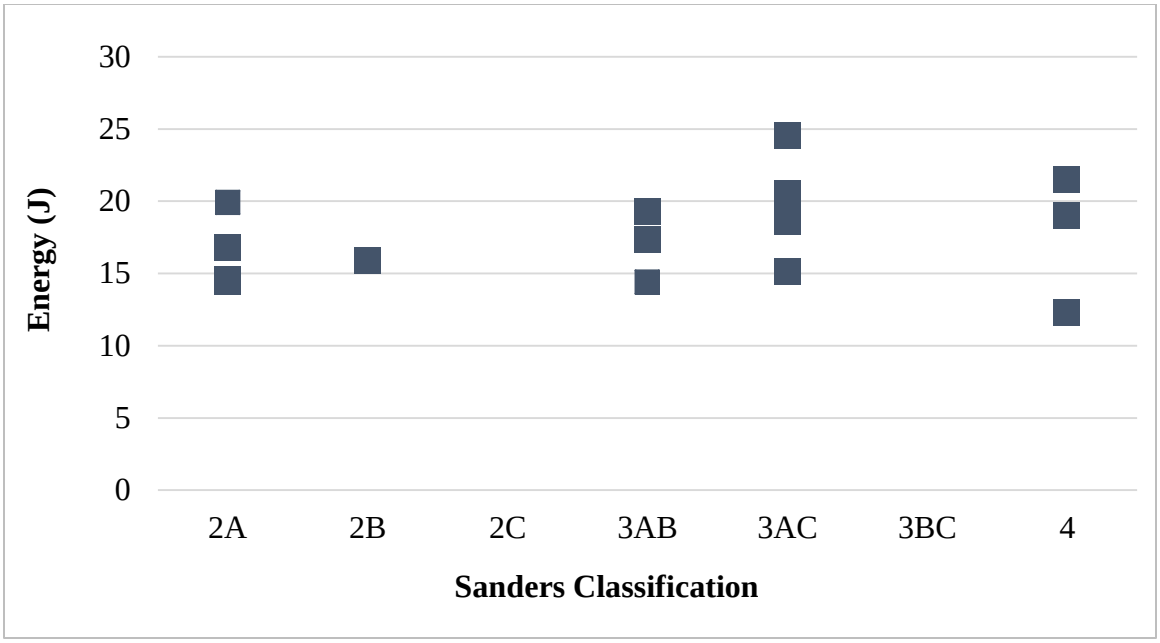

Figure 3-5: Fracture energy vs. Sanders classification subtypes.

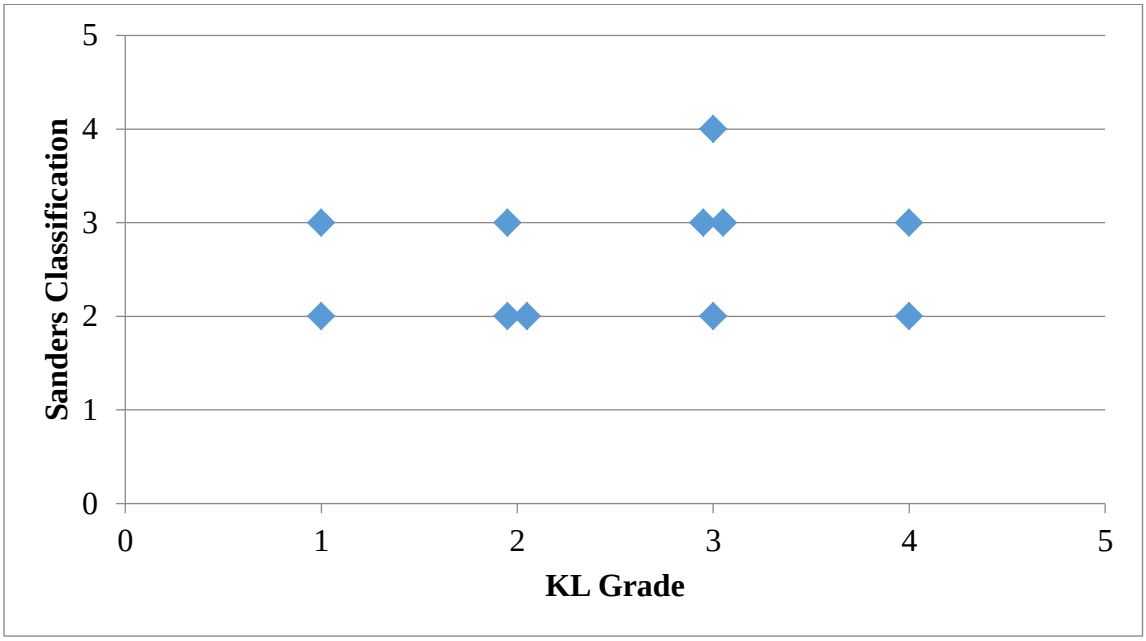

Figure 3-6: Sanders classification vs. KL Grade.

3.6 Comparison:

There were 31 plafond, 61 plateau, and 17 calcaneal fracture cases available for comparison in this study. The range of energies in the tibial plateau fractures was 3.2J to 33.2J with a mean of 13.1J and a standard deviation of 6.8J. The range of fracture energies in the plafond was 3.6J to 26.7J with a mean of 12.9J and a standard deviation of 6.4J. The non-selected series of calcaneal fractures ranged in fracture energy from 12.3J to 24.5J with a mean of 18.1J and a standard deviation of 2.9J. The relative distributions of fracture energies within the plafond and plateau cases were similar. The calcaneal fractures had a narrower range towards the higher end of the energy spectrum for the selected series that were studied.

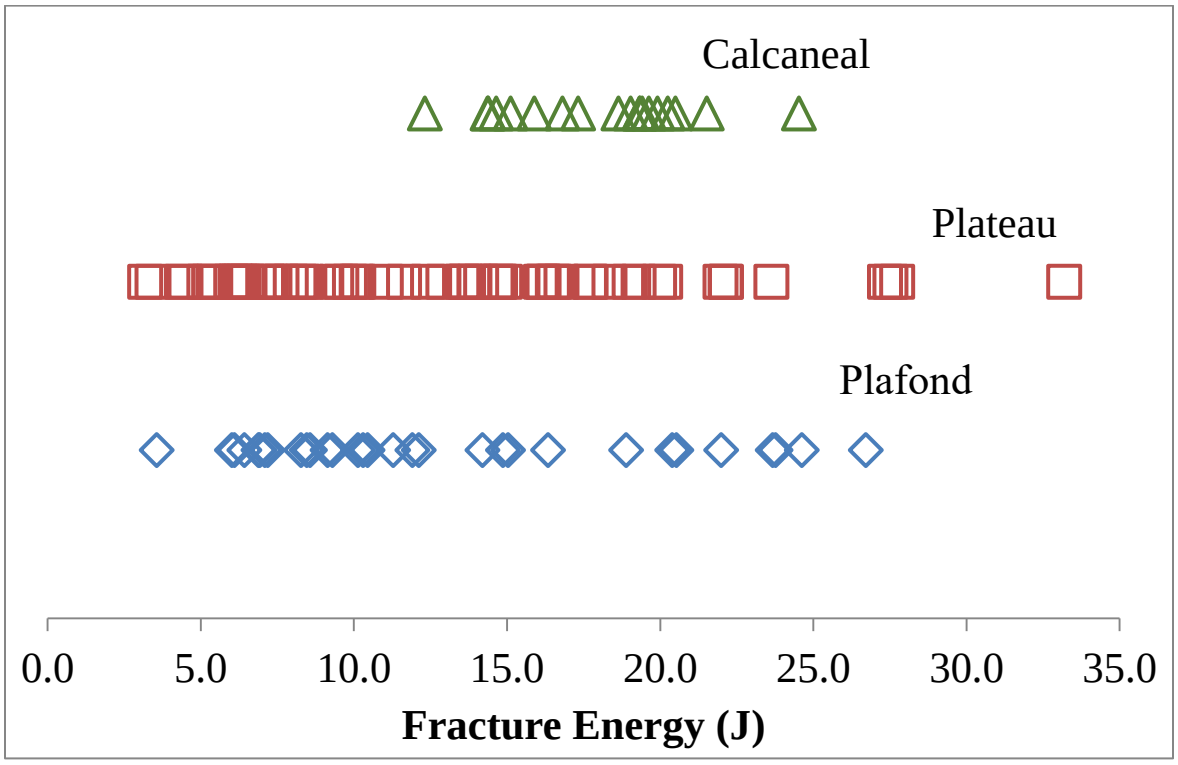

Figure 3-7. Plafond, plateau, and calcaneal fracture energy distributions

CHAPTER 4: Discussion

The primary purpose of the work reported in this thesis was to improve and expand upon existing objective fracture severity assessment techniques. The improvements allowed for the study of a large series of articular fracture cases, which made it possible to evaluate existing clinical injury severity assessment methods. Clinical severity assessments, while having practical utility, have been limited by their inability to scientifically capture characteristics predictive of long term patient outcomes. Previous metrics have identified and implemented objective CT-based techniques that more accurately identify intrinsic factors leading to poor patient outcomes.

Specifically, this study focused on a CT-based technique for objectively quantifying the amount of energy required to produce a fracture in a given bone. This intrinsic factor associated with intra-articular fractures (i.e., fracture energy) is of particular interest as these fractures often have poor outcomes and are typically the result of high energy injury mechanisms. Therefore, it was hypothesized that higher energy fractures would have poorer outcomes. The potential for future clinical application of this hypothesis, allowing for quantitative and objective prediction of patient outcomes, is considerable.

Exploration of potential locations where such a measurements might be most useful is the focus of this discussion. Determining the veracity of new energy metrics' utility in these locations is difficult as there is a paucity of information regarding what components of injury severity are most important. Therefore, when lacking long term

patient follow-up data, the present gold standards for predicting patient outcomes, clinician assessment and clinical severity classification metrics were utilized.

4.1 Fracture Energy Assessment:

The stated goals of the fracture energy assessment were to create a simple, robust, and versatile method for determining the energy involved in a fracture capable of being used in any articular joint. A secondary goal of the work was for the method to operate on a clinically relevant time scale. The simplicity of the method is such that any person able to identify fractures on a CT scan can perform the task. A 3d user interface guides classification of de novo fractured bone area and requires minimal correction in the form of visual inspection of each fractured fragment. Errors found in the classification, like the one shown in figure 2-2, tend to be obvious misclassifications in regions of high curvature. Errors such as these would be expected to be less frequent as the classifier gains access to a larger set of training data moving forward.

The method proved to be robust and versatile as it demonstrated efficacy in the knee, ankle, and subtalar joints. It was capable of working in every case on which it was applied. The secondary goal of operating on a clinically relevant time scale is a point of continuing effort. The method was close to, but ultimately fell short of being consistently under 1 hour. The most time-intensive component, accurate segmentation of fracture fragments, presently requires a significant degree of manual intervention. Fortunately, the time required for this component has the potential to be reduced significantly in future work. The primary objectives of this thesis to create a robust and versatile metric capable of being used in any articular joint were in direct opposition with the time to perform the metric. As all 111 cases in this work were evaluated in respect to clinical measures or

outcomes for research purposes, the segmentations were performed with great attention to detail in fracture fragment identification. Future work will determine the quality and time required for the segmentations to ensure acceptable accuracy in fracture energy evaluation.

4.1.1 Reproducibility

Although no formal study of CT segmentation reproducibility was performed, the same segmentation methods were used in prior work and shown to possess excellent reproducibility. A casual assessment of the reproducibility of segmentations was made using three training segmentation cases performed by two additional analysts. The maximum difference in the fracture energies computed for these cases between different segmentations was around 2 J. The author also noted maximum differences on the order of 2 J for several cases that required reprocessing for various reasons.

4.2 Plateau Rank Ordering:

The fracture energy metric had previously been validated in the tibiotalar joint against clinician assessment by rank ordering cases of varied severity. The next logical application for the energy metric was in the knee with plateau fractures; therefore, the fracture energy was used to rank cases and those rankings were then compared with the present gold standard of subjective expert surgeon rankings, as was done to evaluate the energy metric in the tibial plafond. Inter-user agreement between the six orthopaedic trauma subspecialists was high at 85% concordance. While the level of agreement between the surgeon assessments between fracture severity ranking and energy was not as high at 74%, it was still significantly higher than chance concordance of 50 percent.

There were notable outliers to the trend of concordance between the surgeon assessment and the fracture energy metric. For example, a case ranked the 3rd (6.4 J) on a scale from least to most severe by the fracture energy metric was ranked 10th on average by the surgeons. Another outlier was a case rated the 16th most severe (16.8J) by the energy metric and, 5th on average by the surgeons. Figure 4-1 shows the radiographs rated by the surgeons and the models used in determining the fracture energy for these two cases.

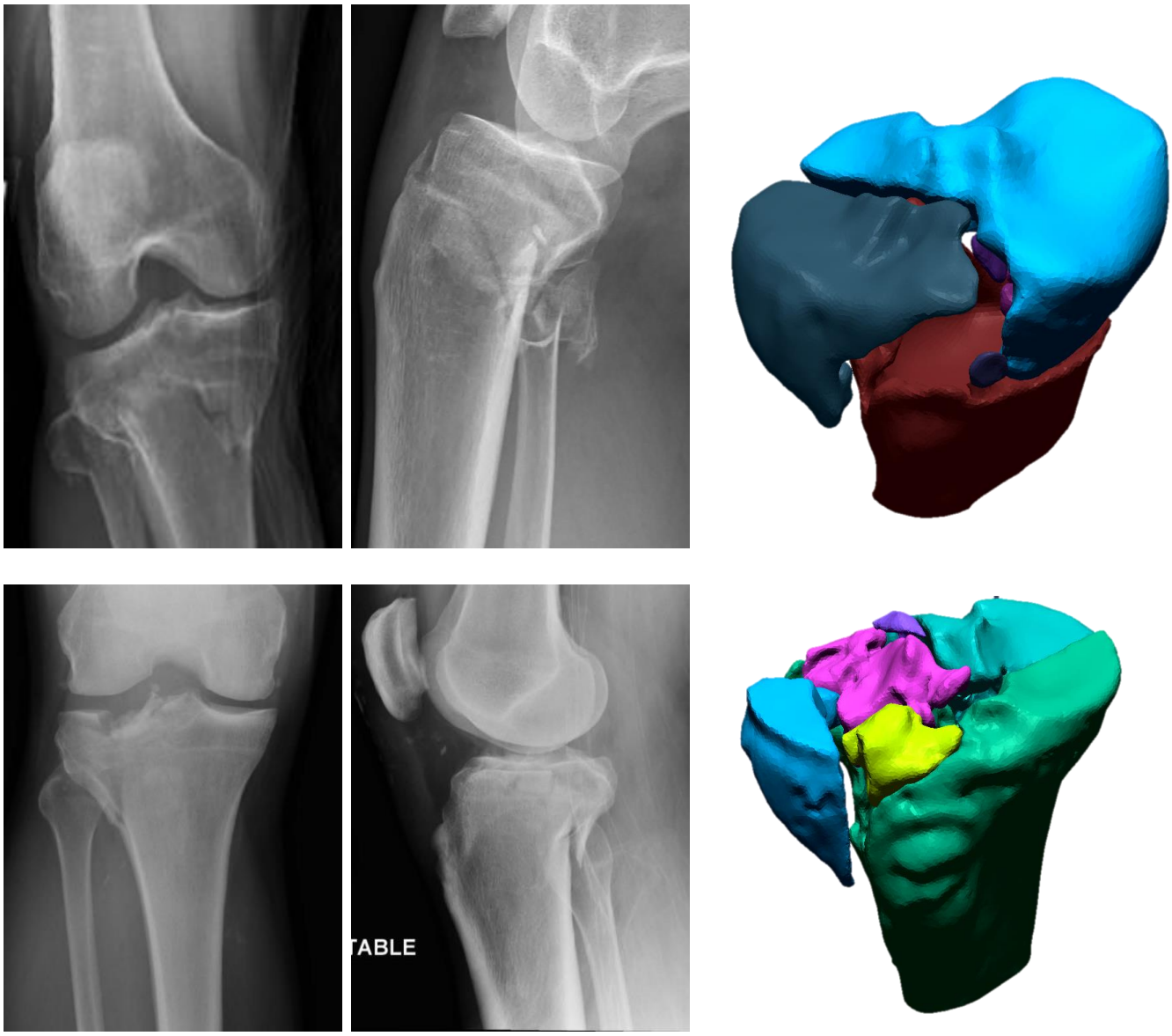

Figure 4-1: Examples of disparate clinician ranking and fracture energy. Top: Low energy 6.4J fracture with high surgeon severity ranking. Bottom: High energy 16.8J fracture with low surgeon severity ranking.

These two cases serve to illustrate important points about the fracture energy metric in comparison with clinician assessment. Patient-specific factors like osteopenia, fracture location, and comminution influence surgeon assessment of injuries but are not directly accounted for by the fracture energy metric. Of these factors, osteopenia is of interest as bone density contributes to the fracture energy measure because the energy absorbed in bone fracture scales directly with density. Lower energies are able to break osteopenic bone more readily due to its lower density. Presently, it is unclear how the fracture energy measure performs against outcomes in such cases, but given its divergence from surgeon ranking, it is possible the fracture energy may be more objectively predictive of outcomes than clinician assessment. However, other patient specific factors mentioned remain unaccounted for and are potential limitations of using only a fracture energy metric to assess severity.

Despite these limitations, fracture energy was shown to have acceptable agreement with expert opinion of injury severity of the entire spectrum of injury severity. Accordingly, the fracture energy metric was shown to have utility in joints other than the plafond. The importance of this result lies in the ability of the metric to quantify an underlying physical property of injuries and use it to objectively assess injury severity. This allows for analysis of a continuous spectrum of injury severity as opposed to a discretized clinical classification that can fail to appreciate subtle differences in fractures. Additionally, the objectivity of employing a calculable physical property prevents clinician bias present in subjective assessments, thereby improving reliability of results.

While the results of this study were promising, it is important to note that surgeon rank ordering does not provide a direct relation to patient outcomes. Therefore, further

investigation will be needed to determine if relationships exist between fracture energy and clinical outcomes. Prior studies in the plafond lend credence to the possibility that such relationships will be found. A 2010 study by Thomas et. al., found fracture energy to be a statistically significant prediction of PTOA at 2 years [10]. Overall, fracture energy in addition to clinician opinion shows strong potential to provide advantages in assessment of injury severity.

4.3 Plateau fracture energy and Schatzker Classification:

Following validation of fracture energy against clinician severity assessment in the tibial plateau, the metric was employed to evaluate the energy metric against the Schatzker classification of plateau fractures. The Schatzker system has well established clinical utility in guiding treatment and predicting outcomes, but its ability to stratify severity had never been assessed. It was designed to identify and group fractures based upon distinct pathomechanical and etiological factors. Additionally, the comparison to fracture energy is also notable due to the potential for further validation of fracture energy metric's predictive capability.

Fractures of the medial plateau (Schatzker IV and V) are typically considered to be more severe than lateral sided (Schatzker I and II) fractures. It might then be hypothesized that medial sided injuries have higher fracture energies, explaining in part the difference in outcomes. The results showed a general monotonically increasing relationship between mean fracture energy and Schatzker classification for the injuries. These results support the hypothesis that differences in outcomes between lateral and medial sided fractures may be explained in part by the initial energy involved with fracturing the joint.

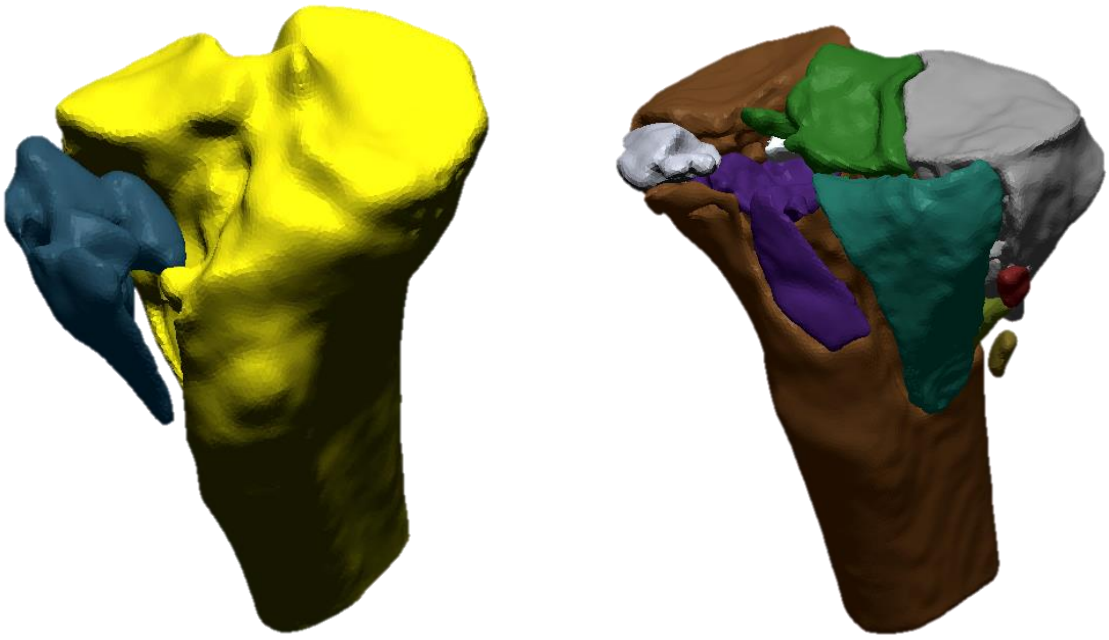

Figure 4-2: Low (left) and high (right) energy Schatzker Class II Fractures.

While the results show a monotonically increasing relationship between fracture energy and Schatzker classification, there was a large degree of overlap between all classes. These findings suggest promising clinical utility for the fracture energy metric in predicting outcomes. Lower energy higher classification fractures may have better outcomes while higher energy lower classification fractures may have worse. Further research into the interplay between Schatzker classification, fracture energy, and patient outcomes is warranted.

4.4 Calcaneal Fracture Energy:

Patients with high-energy intra-articular calcaneal fractures face a poor prognosis with a significant risk of developing PTOA. Prior research has established a link between the energy involved in fracturing the tibial plafond and PTOA, and preliminary results suggest this relationship may exist in other joints. For this reason, the fracture energy metric was applied to high-energy intra-articular calcaneal fractures. It was hypothesized that higher energy calcaneal fractures would have poorer outcomes when compared with relatively lower energy fractures. This is the first opportunity for the fracture energy metric to be compared directly with a patient outcome metric. The Kellgren-Lawrence radiographic arthrosis grading scale or KL grade was chosen as the outcome metric because it offered the most objective metric for outcomes. While it doesn't directly relate to arthritis and arthritic pain, it is a good surrogate for arthritis as the radiographic changes it focuses on can precede pain and further joint degeneration.

The KL-grades of the fractures and the fracture energy metric were both compared with an established clinical metric in calcaneal fractures; the Sanders classification. Previous studies have demonstrated the effectiveness of the Sanders classification as a prognostic marker for long-term clinical outcomes of displaced intra-articular calcaneal fractures [52]. Therefore, associations between the Sanders classification and fracture energy would also be of note.

The results show a very weak association between the KL-grade and the fracture energy. The present clinical classification standard, the Sanders classification, also fails to demonstrate a strong correlation with KL-grade for this small series of cases. However, upon accounting for a known confounder, the post-reduction articular step-off,

a trend emerged. The pre-operative CT scans evaluated for fracture energy showed promise in predicting KL-grade and thus, PTOA development.

When compared to the clinical standard for evaluating calcaneal fractures, the Sanders classification, the objective CT-based fracture energy metric appears to be more predictive of PTOA risk. Residual step-off is likely a confounding variable when evaluating PTOA risk based upon radiographic evidence of PTOA development using the KL grade. It is also important to note that the minimum follow-up time included in this study is 18 months. PTOA is a progressive disease and as such more cases are likely to develop the disease and have poor outcomes and later dates. Additionally, many more cases will likely need to be analyzed before these types of relationships can begin to be adequately understood.

4.5 Fracture Energy Comparison:

While both proximal and distal fractures of the tibia can result in post-traumatic osteoarthritis development, plateau fractures have lower incidence of post-traumatic osteoarthritis when compared with plafond fractures. Reasons for this difference are not well understood, but it is known that differences in outcomes can be related to the acute amount of damage sustained at the time of injury. It stands to reason then that the fracture energy would be higher in the tibial plafond due to the increased incidence of PTOA compared with the plateau. However, the results do not support such a hypothesis. There was no discernable difference in the fracture energy range between the two fracture types. Thus, other factors exist that need to be considered upon interpretation of the results.

A major confounder stems from the quality of surgical reduction. Offsets in the joint congruity larger than 2 mm have been demonstrated to increase risk of PTOA at 2 years in the tibial plafond. However, the tibial plateau is thought to be generally more accepting of articular step-offs showing no statistically significant difference in outcomes in fractures with <3 mm of displacement [53]. This obfuscates the relationship between fracture energy and patient outcomes as articular step-off is shown to be an independent predictor of the differences in PTOA rates between the plafond and plateau. Further complicating this relationship is the fact that higher energy fractures typically have more complex fracture patterns and a greater degree of comminution. Both of which can make accurate surgical reductions more challenging thus resulting in larger step-offs. Therefore, the energy of the fractures may be predictive of the step-off which may be the true cause of observed differences in PTOA rates.

Further complicating the relationship are the differences in joint anatomy. The plafond injuries may simply be more difficult to accurately reduce to than plateau injuries. Other potential differences could stem from the size of the anatomy. The tibial plateau has a significantly larger articulating surface (1150 mm^2) than the tibial plafond (578±83 mm^2) [54, 55]. The joint therefore, could experience a higher energy per unit area transmitted upon fracturing leading to poorer outcomes.

Substantial differences in soft tissue structures also offer an anatomical explanation. The tibial plateau has a dense, load bearing, fibrocartilaginous meniscus and substantial soft tissue. It is reasonable to assume that in contrast with the robust bony load bearing in the ankle, the knee's soft tissues aid in preventing its degradation post-fracture despite similar energies involved in the injuries.

Calcaneal fractures included in this study were not chosen to span the spectrum of injury and only included Sanders class 2 through 4 injuries. Sanders classes 2 through 4 fractures are generally considered very severe injuries and thus, it was anticipated that the energy spectrum these injuries spanned would be smaller and higher in comparison to the tibial injuries. The results showed that the injuries observed did not span a large distribution of fracture energies and were focused on the higher end of the energy spectrum as anticipated.

The calcaneus is a relatively small, dense bone in comparison to the tibia. Therefore, it is possible that there is a lower ceiling or a higher floor for fracture energy in calcaneal injuries. Ongoing study of calcaneal fractures spanning a larger spectrum of injuries will enable a more complete picture of whether differences such as these exist between fractures of different bones and joints.

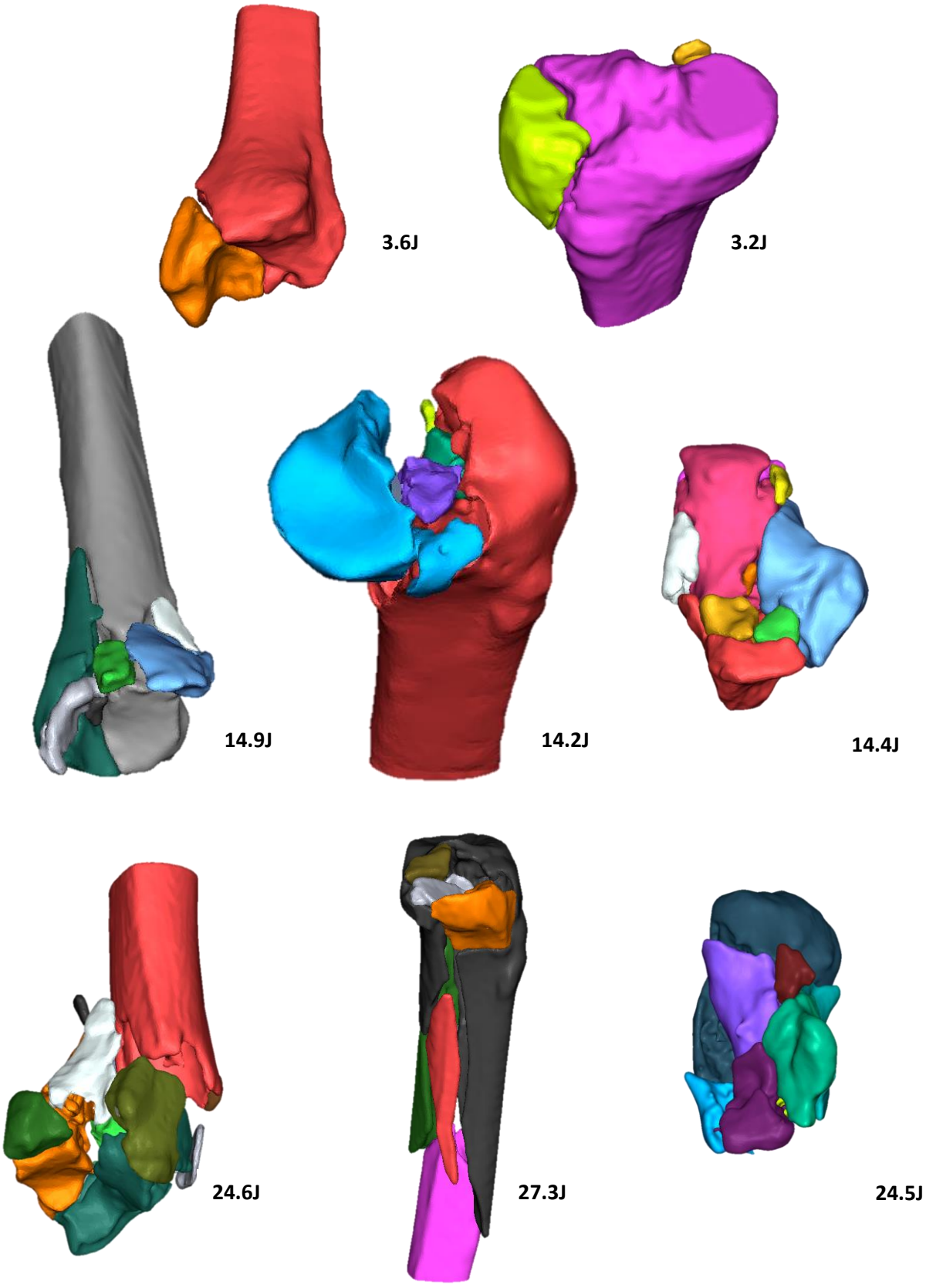

Figure 4-3: Fracture energy comparison between tibial plafond (left), plateau (middle), and calcaneal (right) injuries.

4.6 Limitations:

The methodology described in this work is not without limitations. Unlike the prior fracture energy work, the new methodology does not yet include an articular comminution metric. The articular comminution metric used previously combined with the fracture energy demonstrated excellent predictive capabilities. Additionally, in clinician evaluation of severity ranking for the plateau, orthopaedic surgeons judged the fracture severity based upon plain radiographs, and not on the CT scan data with which the fracture energy was evaluated. Therefore, it is possible that there were fracture characteristics that were not appreciated on the plain radiographs. This could have led to an underestimation of severity by surgeon assessment.

Further limitations stem from the speed and assumptions implicit in the methodology. Each fracture severity assessment required approximately 1 hour to complete. A vast majority of this time required significant user interaction in the segmentation and classification tasks. While it was faster than the previous fracture energy methodology's 8-10 hour evaluation, it failed to achieve the speed (~15 minutes per fracture) of the previously expedited method. An invalid assumption inherent to the energy calculation is that bone is a brittle solid. Thus, this method does not account for any plastic deformation that might occur. Hence, impaction fractures may have absorbed energy not accounted for in the metric that lead to underestimation of injury severity.

4.7 Conclusions:

This thesis detailed the development of a fracture severity assessment methodology capable of being applied to any articular fracture. The methods were designed to reliably and objectively determine a physically meaningful property of fractures, the energy absorbed by the bone upon fracturing. It demonstrated substantial improvements over prior fracture energy assessment work. These improvements included reducing the time from 8-10 hours down to ~1 hour per case and more accurately representing fractured area energy release rates. The newly developed fracture severity assessment methods proved capable as a versatile gauge of injury severity in multiple joints. It was tested against clinician assessment in the tibial plateau and plafond, and was evaluated against present clinical severity systems in the plateau, plafond, and calcaneus. It demonstrated good agreement with both clinician assessment and clinical severity classification systems. It also demonstrated predictive capabilities in calcaneal fractures for patient outcomes. In conclusion, while the objective CT-based measurement of fracture energy showed promise, ongoing work will determine the extent of its clinical utility.

4.8 Future Directions:

Future directions for this work include implementing additional physically meaningful objective measures of injury severity. One such measure could be of the articular fracture edge length. The 3d interface of the fracture classification system presented in this work as well as boundaries between the fractured and intact bone could be leveraged to identify fractures along the articular surface and quantify their length. This is meaningful as it is known that chondrocyte death is elevated along articular fracture edges [56]. This chondrocyte death and therefore fracture edge length have the potential be useful in prediction of PTOA. Additional physical measures with such potential also exist like the degree of articular comminution and the amount of fragment displacement. Objective quantification and combination of these measures offers promising future research directions.

Another promising area for improvement is in the segmentation task. Segmentation and model creation required ~75% of the time spent on each case to complete. This leaves potential for substantial increases in the speed of metric evaluation when coupled with continually improving classification training sets. The ultimate goal of such improvements would be to achieve clinically relevant analysis on a clinically relevant time scale. Thus, allowing clinicians to have access to the energies involved in patient injuries helping to guide assessment of injury severity.

REFERENCES

1. *Gaussian Curvature.* Wikipedia, The Free Encyclopedia, 2015.
2. Badillo, K., et al., *Multidetector CT evaluation of calcaneal fractures.* Radiographics, 2011. **31**(1): p. 81-92.
3. Thomas, T.P., *Development and Implementation of CT-based Measures for Objective Fracture Severity Assessment.* University of Iowa, 2007.
4. Anderson, D.D., et al., *Quantifying tibial plafond fracture severity: absorbed energy and fragment displacement agree with clinical rank ordering.* J Orthop Res, 2008. **26**(8): p. 1046-52.
5. Thomas, T.P., et al., *A method for the estimation of normative bone surface area to aid in objective CT-based fracture severity assessment.* Iowa Orthop J, 2008. **28**: p. 9-13.
6. Beardsley, C.L., et al., *Interfragmentary surface area as an index of comminution severity in cortical bone impact.* J Orthop Res, 2005. **23**(3): p. 686-90.
7. Swiontkowski, M.F., et al., *Interobserver variation in the AO/OTA fracture classification system for pilon fractures: is there a problem?* J Orthop Trauma, 1997. **11**(7): p. 467-70.
8. Walton, N.P., et al., *AO or Schatzker? How reliable is classification of tibial plateau fractures?* Arch Orthop Trauma Surg, 2003. **123**(8): p. 396-8.
9. Müller, M.E., *The comprehensive classification of fractures of long bones*. 1990, Berlin ; New York: Springer-Verlag. xiii, 201 p.
10. Thomas, T.P., et al., *Objective CT-based metrics of articular fracture severity to assess risk for posttraumatic osteoarthritis.* J Orthop Trauma, 2010. **24**(12): p. 764-9.
11. Kilburg, A.T., *Development of an expedited objective fracture severity assessment methodology.* University of Iowa, 2012.
12. Saltzman, C.L., et al., *Impact of comorbidities on the measurement of health in patients with ankle osteoarthritis.* J Bone Joint Surg Am, 2006. **88**(11): p. 2366-72.
13. Weigel, D.P. and J.L. Marsh, *High-energy fractures of the tibial plateau. Knee function after longer follow-up.* J Bone Joint Surg Am, 2002. **84-A**(9): p. 1541-51.
14. Marsh, J.L., D.P. Weigel, and D.R. Dirschl, *Tibial plafond fractures. How do these ankles function over time?* J Bone Joint Surg Am, 2003. **85-A**(2): p. 287-95.
15. Anderson, D.D., J.L. Marsh, and T.D. Brown, *The pathomechanical etiology of post-traumatic osteoarthritis following intraarticular fractures.* Iowa Orthop J, 2011. **31**: p. 1-20.
16. Anderson, D.D., et al., *Post-traumatic osteoarthritis: improved understanding and opportunities for early intervention.* J Orthop Res, 2011. **29**(6): p. 802-9.
17. Anderson, D.D., et al., *Is elevated contact stress predictive of post-traumatic osteoarthritis for imprecisely reduced tibial plafond fractures?* J Orthop Res, 2011. **29**(1): p. 33-9.
18. Flandry, F. and G. Hommel, *Normal anatomy and biomechanics of the knee.* Sports Med Arthrosc, 2011. **19**(2): p. 82-92.
19. Blackburn, T.A. and E. Craig, *Knee anatomy: a brief review.* Phys Ther, 1980. **60**(12): p. 1556-60.
20. Stockman, T.J., *Early Targeting of Knee Osteoarthritis: Validation of Computational Methods.* University of Iowa, 2014.
21. *Knee.* National Sports Medicine Institute, 2007.
22. Hohl, M., *Managing the Challenge of Tibial Plateau Fractures.* J Musculoskeletal Med, 1991(8): p. 70-86.

23. Kilstrup, M., *Naturalizing semiotics: The triadic sign of Charles Sanders Peirce as a systems property.* Prog Biophys Mol Biol, 2015.
24. Schatzker, J., R. McBroom, and D. Bruce, *The tibial plateau fracture. The Toronto experience 1968--1975.* Clin Orthop Relat Res, 1979(138): p. 94-104.
25. Rademakers, M.V., et al., *Operative treatment of 109 tibial plateau fractures: five- to 27-year follow-up results.* J Orthop Trauma, 2007. **21**(1): p. 5-10.
26. Marsh, J.L., et al., *Fracture and dislocation classification compendium - 2007: Orthopaedic Trauma Association classification, database and outcomes committee.* J Orthop Trauma, 2007. **21**(10 Suppl): p. S1-133.
27. Berkson, E.M. and W.W. Virkus, *High-energy tibial plateau fractures.* J Am Acad Orthop Surg, 2006. **14**(1): p. 20-31.
28. P.de Boer, R.M., *(iv) Pilon fractures of the Tibia.* Current Orthopaedics, 2003. **17**(3): p. 190-199.
29. Bourne, R.B., C.H. Rorabeck, and J. Macnab, *Intra-articular fractures of the distal tibia: the pilon fracture.* J Trauma, 1983. **23**(7): p. 591-6.
30. Porter, M.C.a.K., *The pilon fracture.* Trauma, 2010. **12**: p. 89-103.
31. Mast, J.W., P.G. Spiegel, and J.N. Pappas, *Fractures of the tibial pilon.* Clin Orthop Relat Res, 1988(230): p. 68-82.
32. Williams, T.M., et al., *Factors affecting outcome in tibial plafond fractures.* Clin Orthop Relat Res, 2004(423): p. 93-8.
33. Browner, B.D., et al., *Skeletal trauma basic science, management, and reconstruction*. p. 1 online resource.
34. Ruedi, T.P. and M. Allgower, *The operative treatment of intra-articular fractures of the lower end of the tibia.* Clin Orthop Relat Res, 1979(138): p. 105-10.
35. Hall, R.L. and M.J. Shereff, *Anatomy of the calcaneus.* Clin Orthop Relat Res, 1993(290): p. 27-35.
36. Sarrafian, S.K., *Biomechanics of the subtalar joint complex.* Clin Orthop Relat Res, 1993(290): p. 17-26.
37. Bajammal, S., et al., *Displaced intra-articular calcaneal fractures.* J Orthop Trauma, 2005. **19**(5): p. 360-4.
38. Griffin, D., et al., *Operative versus non-operative treatment for closed, displaced, intra-articular fractures of the calcaneus: randomised controlled trial.* BMJ, 2014. **349**: p. g4483.
39. Sanders, R., *Intra-articular fractures of the calcaneus: present state of the art.* J Orthop Trauma, 1992. **6**(2): p. 252-65.
40. Sanders, R., et al., *The Operative Treatment of Displaced Intra-articular Calcaneal Fractures (DIACFs): Long Term (10-20 years) Results in 108 Fractures using a Prognostic CT Classification.* J Orthop Trauma, 2014.
41. Beardsley, C.L., et al., *Interfragmentary surface area as an index of comminution energy: proof of concept in a bone fracture surrogate.* J Biomech, 2002. **35**(3): p. 331-8.
42. Borrelli, J., Jr. and W.M. Ricci, *Acute effects of cartilage impact.* Clin Orthop Relat Res, 2004(423): p. 33-9.
43. Langley., G.H.J.a.P., *Estimating continuous distributions in bayesian classifiers.* Eleventh Conference on Uncertainty in Artificial Intelligence., 1995.
44. Vangelis M., I.A., and Geogios P., *Spam Filtering with Naive Bayes - Which Naive Bayes?* . Third Conference on Email and Anti-Spam., 2006.
45. Mitchell, T., *Machine Learning.* McGraw Hill, 1997.

46. Morvan., D.C.-S.a.J.-M., *Restricted Delaunay triangulations and normal cycle.* In Proc. 19th Annual ACM Symposium on Computational Geometry, 2003: p. 237-246.
47. Pierre Alliez, D.C.-S., Olivier Devillers, Bruno LeŽvy, and Mathieu Desbrun., *Anisotropic Polygonal Remeshing. .* ACM Transactions on Graphics, 2003.
48. Boykov, Y. and V. Kolmogorov, *An experimental comparison of min-cut/max-flow algorithms for energy minimization in vision.* IEEE Trans Pattern Anal Mach Intell, 2004. **26**(9): p. 1124-37.
49. Snyder, S.M. and E. Schneider, *Estimation of mechanical properties of cortical bone by computed tomography.* J Orthop Res, 1991. **9**(3): p. 422-31.
50. Thomas, T.P., *Virtual Pre-Operative Reconstruction Planning for Comminuted Articular Fractures.* University of Iowa, 2010.
51. Kellgren, J.H. and J.S. Lawrence, *Radiological assessment of osteo-arthrosis.* Ann Rheum Dis, 1957. **16**(4): p. 494-502.
52. Sanders, R., et al., *Operative treatment of displaced intraarticular calcaneal fractures: long-term (10-20 Years) results in 108 fractures using a prognostic CT classification.* J Orthop Trauma, 2014. **28**(10): p. 551-63.
53. Honkonen, S.E., *Indications for surgical treatment of tibial condyle fractures.* Clin Orthop Relat Res, 1994(302): p. 199-205.
54. Fukubayashi, T. and H. Kurosawa, *The contact area and pressure distribution pattern of the knee. A study of normal and osteoarthrotic knee joints.* Acta Orthop Scand, 1980. **51**(6): p. 871-9.
55. Li, W., et al., *Patient-specific finite element analysis of chronic contact stress exposure after intraarticular fracture of the tibial plafond.* J Orthop Res, 2008. **26**(8): p. 1039-45.
56. Lewis, J.L., et al., *Cell death after cartilage impact occurs around matrix cracks.* J Orthop Res, 2003. **21**(5): p. 881-7.